Modeling Dark Matter and Dark Energy

Kevin J. Ludwick

A dissertation submitted to the faculty of the University of North Carolina at Chapel Hill in partial fulfillment of the requirements for the degree of Doctor of Philosophy in the Department of Physics and Astronomy.

Chapel Hill
2013

Approved by:

Y. Jack Ng

Charles R. Evans

Reyco Henning

Dmitri Khveshchenko

Robert J. Scherrer

© 2013
Kevin J. Ludwick
ALL RIGHTS RESERVED

Abstract

KEVIN J. LUDWICK: Modeling Dark Matter and Dark Energy.
(Under the direction of Paul H. Frampton.)

We study various models of dark matter and dark energy. We first examine the implications of the assumption that black holes act as dark matter. Assuming dark matter in galactic halos is composed solely of black holes, and using observational constraints, we calculate the number of halo black holes and the total entropy due to them. We then study the prospect of dark energy with a non-constant density. We analyze several parameterizations of dark energy density from the literature and one of our own, in particular focusing on the value of redshift at which cosmic acceleration due to dark energy begins. In considering the properties of dark energy densities that monotonically increase over time, we present two new categorizations of dark energy models that we dub "little rip" and "pseudo-rip" models, and both avoid future singularities in the cosmic scale factor. The dark energy density of a little rip model continually increases for all future time, and a pseudo-rip model's dark energy density asymptotically approaches a maximum value. These two types of models, big rip models, and models that have constant dark energy densities comprise all categories of dark energy density with monotonic growth in the future. A little rip leads to the dissociation of all bound structures in the universe, and a pseudo-rip occurs when all bound structures at or below a certain threshold dissociate. We present explicit parameterizations of the little rip and pseudo-rip models that fit supernova data well, and we calculate the times at which particular bound structures rip apart. In looking at different applications of

these models, we show that coupling between dark matter and dark energy with an equation of state for a little rip can change the usual evolution of a little rip model into an asymptotic de Sitter expansion. We also give conditions on minimally coupled phantom scalar field models and scalar-tensor models that indicate whether or not they lead to a little rip or a pseudo-rip.

Acknowledgments

I am grateful to my advisor, Paul Frampton, for all his dedication, guidance, and help throughout graduate school. I am thankful for all the members of my committee and the work they have done. I am also grateful to Robert Scherrer for his collaboration in research and all the help he has offered me. I thank Shin'ichi Nojiri and Sergei Odintsov for their collaboration in research. I appreciate all that Jack Ng, Chris Clemens, and the rest of the physics department have done for me.

Many thanks to Mom, Dad, Jessica, Ryan, Nathan, and the rest of my family for all their love, support, and good advice. I appreciate the long-time friendship of Lee, Philip, and my apartment-mate Jeremy. I would not have eaten nearly as well as I have over the past five years had it not been for the love, friendship, and and excellent cooking of the Seniors (my second family), Teresa, the Tarltons, and the Cuanies. And to others I did not mention here, thank you.

Table of Contents

List of Figures . . . . . **viii**

List of Tables . . . . . **ix**

1 Introduction **1**

1.1 Historical Background 1

1.2 Overview of Dark Matter and Dark Energy 5

1.3 Motivation and Plan of this Work 12

2 Number and Entropy of Black Holes **18**

2.1 Introduction 18

2.2 Number of Black Holes 19

2.3 Entropy of Black Holes 21

2.4 Reconsideration of the Entropy of the Universe 23

3 Seeking Evolution of Dark Energy **26**

3.1 Introduction 26

3.2 Evolutionary Dark Energy Models 28

3.3 Analysis of the Models 29

3.4 Slowly Varying Criteria 34

3.5 Discussion and Conclusions 35

4 The Little Rip . . . 38

4.1 Introduction . . . 38

4.2 The Conditions for a Future Singularity . . . 39

4.3 Constraining Little Rip Models . . . 45

4.4 Disintegration . . . 46

4.5 Discussion . . . 49

5 Models for Little Rip Dark Energy . . . 51

5.1 Introduction . . . 51

5.2 Inertial Force Interpretation of the Little Rip . . . 52

5.3 Coupling with Dark Matter . . . 58

5.4 Scalar Field Little Rip Cosmology . . . 62

5.4.1 Minimally Coupled Phantom Models . . . 62

5.4.2 Scalar-Tensor Models . . . 63

5.5 Including Matter . . . 67

5.6 Discussion . . . 69

6 The Pseudo-Rip . . . 71

6.1 Introduction . . . 71

6.2 Definition of Pseudo-Rip . . . 72

6.3 Model 1 . . . 75

6.4 Model 2 . . . 78

6.5 Scalar Field Realizations . . . 79

6.6 Discussion . . . 80

7 Conclusions and Future Directions . . . 83

Bibliography . . . 86

List of Figures

3.1 $w_0^{(lin)}$ vs. $w_1^{(lin)}$ 30

3.2 $w_0^{(CPL)}$ vs. $w_1^{(CPL)}$ 31

3.3 $w_0^{(SSS)}$ vs. $w_1^{(SSS)}$ 31

3.4 $w_0^{(new)}$ vs. $w_1^{(new)}$ 32

3.5 $w(Z)$ vs. Z for all models 33

4.1 Hubble plot and Hubble residual plot 47

6.1 Scaled F_{inert} for Model 1 77

6.2 Scaled F_{inert} for Model 2 79

List of Tables

2.1 Number of black holes with constraints from wide binaries 20
2.2 Number of black holes without constraints from wide binaries 21
2.3 Entropy of black holes with constraints from wide binaries 22
2.4 Entropy of black holes without constraints from wide binaries 22

Chapter 1

Introduction

1.1 Historical Background

Our universe is mysterious and wonderful. As we plumb deeper the depths of space with our detectors and telescopes, the more we find that we do not understand. Modern cosmology, the study of our universe's origins, structure, dynamics, and ultimate fate, has dramatically evolved from what it was in the early 1900s to what it is today.

Soon after Einstein published his tensor equation describing general relativity in 1915, he applied his equation to the universe in 1917, giving birth to relativistic cosmology. His equation implied that the universe was expanding, and this description did not agree with the popular conception of the universe during his day. So he added an extra term, often called the cosmological constant term, that was consistent with the derivation of his equation, and this extra term ensured that his equation described the universe as static [1]. As it turns out, the addition of the cosmological constant term gives a quasistatic solution that is unstable under perturbations. Alexander Friedmann [2] and Georges Lemaître [3] independently wrote down the solution to Einstein's equation for a homogeneous and isotropic universe (which is an accurate description of our universe on a large scale). Lemaître

realized that the solution gave a universe that started from a singularity. His realization was the origin of the big bang theory, and it was not a widely accepted one at that time. Later, Howard Percy Robertson [4] and Arthur Geoffrey Walker [5], working independently in the 1930s, also worked out the solution for such a universe. Their eponymous metric, the Friedmann-Lemaître-Robertson-Walker (FLRW) metric, is the standard metric used in modern cosmology. Lemaître [3] in 1927 and Edwin Hubble [6] in 1929, based on data from recession velocities of galaxies, showed that the universe was, in fact, expanding. Hubble plotted the recessional velocities of a set of galaxies versus their distance away from us, and he made a linear fit. He deduced what is known as Hubble's Law: $v = H_0 d$, where v is the velocity, d is the distance, and H_0 is the constant slope, known as Hubble's constant. The recessional velocity of galaxies and their distances away from us are not related by a constant in time in general, but for the set of nearby galaxies Hubble observed, a linear relationship with a constant slope of H_0 is fairly accurate. The idea of the big bang gained more popularity because of this evidence of expansion. Einstein later said that adding the cosmological constant term to avoid expansion was his biggest mistake. However, it turns out that the cosmological constant is quite useful in describing dark energy, which we will discuss soon.

In response to the discovery of universal expansion, an alternative to the big bang theory was proposed in the 1920s by Sir James Jeans, and his theory was called the steady-state theory. In a steady-state universe, the universe has no beginning or end, and new matter is continuously generated as the universe expands. The FLRW metric follows the cosmological principle, which says that the universe is homogeneous and isotropic on a large scale in space, but structure changes over time as the universe expands. The steady-state universe follows the perfect cosmological principle, which says that the universe is homogeneous and isotropic in

space *and* in time. So a steady-state universe does not change its appearance over time. In 1948, a revised version of the steady-state model was promulgated by Fred Hoyle, Thomas Gold, and Herman Bondi, among others. However, evidence against this theory cropped up in the 1960s. Quasars and radio galaxies that were far away from our galaxy were observed, but none were seen that were close to us. This was a violation of the perfect cosmological principle.

For most, the final blow to the steady-state theory was the discovery of the cosmic microwave background (CMB). In 1965, Arno Penzias and Robert Wilson published their discovery of a uniform background of microwave radiation [7]. They had built a Dicke radiometer intended for experiments for satellite communication. They discovered an excess in their antenna's temperature that was independent of the its orientation, and it was due to the CMB. The steady-state model predicted discrete sources of background radiation from distant stars, but the CMB gives off an almost perfectly uniform, blackbody spectrum. However, the big bang theory very nicely predicts the existence of a microwave background of radiation due to the decoupling of photons from electrons and protons as the universe cooled over time. In fact, Ralph Alpher and Robert Herman predicted in 1948 a cosmic microwave background of $5\ \mathrm{K}$ [8], which is close to the modern experimental value of $2.72548 \pm 0.00057\ \mathrm{K}$ [9]. The CMB is not perfectly uniform; however, the anisotropies, which provide valuable insight into the formation of our early universe and its structure, are well predicted by the big bang model when augmented by inflation and quantum fluctuations of the inflaton field.

Shortly after the expansion of the universe was confirmed, Fritz Zwicky noticed a discrepancy between mass measurements of galaxies in the Coma Cluster in 1933. There was not enough luminous matter to account for the observed galactic velocities near the edge of the cluster according to the virial theorem, so he

concluded that there was missing mass, "dark matter," that accounted for the unexpected observations [10]. In the 1960s and 1970s, Vera Rubin and others used a new spectrograph that measured more accurately than ever before the rotation curves of spiral galaxies, which show how fast stars orbit around the centers of galaxies. Like Zwicky, she found an apparent violation of the virial theorem. The stars near the edge of the spiral galaxies she observed were moving too fast to stay bound to their galaxies according to the galactic masses measured from the visible matter in them. In fact, she showed that about 50% of a typical spiral galaxy's mass is located beyond the radius containing the luminous galactic matter. She and her collaborators published their results in 1980 [11].

Another milestone in cosmology recently happened when the High-z Supernova Search Team in 1998 [12] and the Supernova Cosmology Project in 1999 [13] published observations of the emission spectra of Type Ia supernovae indicating that the universe's rate of outward expansion is increasing. These groups found that supernovae exhibited emission spectra that were redshifted more than expected from supernovae in a decelerating or zero-acceleration universe, so they inferred that the universe was accelerating. Galaxy surveys and the late-time integrated Sachs-Wolfe effect also give evidence for the universe's acceleration. Thus, "dark energy" was proposed as the pervasive energy in the universe necessary to produce the "anti-gravitational," outward force that causes this acceleration, which has been observationally tested and vetted since its discovery. The 2011 Nobel Prize in Physics was awarded to Schmidt, Riess, and Perlmutter for their pioneering work leading to the discovery of dark energy.

1.2 Overview of Dark Matter and Dark Energy

About twenty-four percent of our universe is composed of dark matter, matter that is electromagnetically undetectable because it does not emit any observable amount of light. However, this non-luminous matter has been detected gravitationally via gravitational lensing, and anisotropies in the CMB, examination of baryonic acoustic oscillations (BAO), and structure formation simulations provide good support for its existence.

Because dark matter is non-luminous, it is electromagnetically neutral. It is also safe to say that particulate dark matter is not completely made up of baryonic particles; otherwise, the CMB and comic structure formation would be drastically different. Observational constraints on light elements created during big bang nucleosynthesis, which strongly depend of baryon abundance [14], conflict with such a theory. (There is some room for baryonic dark matter in the form of massive compact halo objects (MACHOs), which will be discussed later.) Dark matter cannot be completely composed of "hot" particles, meaning particles that travel at relativistic speeds. Light particles travel at ultrarelativistic speeds in the early universe and stream through density perturbations, dampening them. One can relate the smallest scale at which there is clumpy dark matter to the particle's mass. Lyman-α constraints suggest that a dark matter particle's mass should be ≥ 2 keV [15].

There are many posited candidates for dark matter. Probably the most popular candidate for cold (non-relativistic) dark matter is the Weakly Interacting Massive Particle (WIMP). Such a particle was first proposed by Steigman and Turner [16], and it interacts and has mass that is at the weak interaction scale. If such particles are in a thermal bath in the early universe and have an annihilation cross section at the weak scale, the number density obtained by solving the Boltzmann

equation agrees with the observational value for the number density of dark matter [17]. Some examples of WIMPs are the neutralino (motivated from supersymmetry) and the Kaluza-Klein photon (motivated from theories with extra dimensions). Other dark matter candidates include axion (proposed particles that solve the strong CP problem), supersymmetric gravitinos, and dark matter from the hidden sector, which is a theoretical extension to the Standard Model comprised of fields that have very little interaction with fields in the Standard Model. Another candidate for dark matter is the leading warm dark matter candidate, the sterile neutrino. Proponents argue that this model leads to more accurate structure formation than cold dark matter does [18, 19]. Typical examples of the aforementioned MACHOs, which were originally proposed as objects that explained the presence of non-luminous matter in galaxy halos, include neutron stars and black holes. Primordial black holes (PBHs) and ultra-compact minihalos (UCMHs) are more recent dark matter candidates. They may be classified as non-baryonic MACHOs, and they form via the collapse of density perturbations near the time of the big bang [20, 21, 22].

Instead of accounting for dark matter with extra matter, we can also try modified gravity models (e.g., $f(R)$ gravity, scalar-tensor theories, Brans-Dicke theories, braneworld gravity). Another attempt of modifying gravitational laws is called Modified Newtonian Dynamics (MOND). The challenge for such models is to correctly describe both structure formation and galaxy rotation curves. For example, MOND is consistent with galaxy rotation curves, but it has more trouble with structure formation.

It is a bit surprising that the amount of baryonic matter in the universe is dwarfed by six times as much dark matter. Perhaps even more unsettling is the presence of dark energy in our universe, which makes up the biggest portion,

about three quarters, of our universe.

However, our physical intuition of the nature and dynamics of dark energy is severely lacking. For a fixed amount of normal matter, as the volume containing it increases, the density of the matter for the whole volume should decrease. However, the nature of dark energy is counterintuitive in that its density remains constant (or even increases) over time as the universe expands.

Many explanations for cosmic acceleration have been theorized. The varied approaches include modified gravity, adding an extra component for dark energy to the components of mass/energy in the universe, and cosmological back-reaction, which refers to the scenario in which inhomogeneity in the universe accounts for cosmic acceleration. The standard explanation attributes dark energy to vacuum energy that permeates the universe and is constant over time. The model that accompanies this explanation is called the cosmological constant model, named after the extra term Einstein added into his equation to give a static universe. Einstein's equation can be derived with an extra term that is a constant times the metric (the speed of light $c = 1$ throughout):

$$R_{\mu\nu} - \frac{1}{2}Rg_{\mu\nu} + \Lambda g_{\mu\nu} = 8\pi G T_{\mu\nu}. \tag{1.1}$$

$R_{\mu\nu}$ is the Ricci tensor, R is the Ricci scalar (the contracted Ricci tensor), $g_{\mu\nu}$ is the metric, and $T_{\mu\nu}$ is the stress-energy tensor, which contains all the information about the mass/energy contents of spacetime. The first two terms on the lefthand side of the equation are the usual terms from Einstein's equation representing the curvature of spacetime. The third, extra term is the contribution of vacuum dark energy, and the constant multiplier, Λ, is called the cosmological constant. Quantum field theory predicts a value for the vacuum energy that disagrees with the experimental

cosmological value by an appalling 120 orders of magnitude, the largest discrepancy between theory and experiment in all of physics. Perhaps the correct theory of quantum gravity or some other theory will explain this inconsistency, and many explanations have been proffered, for example, based on the string landscape and the anthropic principle. It is a mystery for now.

The FLRW metric, mentioned previously, is

$$ds^2 = -dt^2 + a(t)^2 \left[\frac{dr^2}{1 - kr^2} + r^2(d\theta^2 + \sin^2\theta d\phi^2) \right], \tag{1.2}$$

where $a(t)$ is the scale factor controlling the rate at which the universe expands/contracts, and k determines the spatial curvature of the universe. Observations have shown that the universe is almost completely spatially flat, i.e., k is very close to 0, so it is usually set to 0 (and we use $k = 0$ throughout this work unless otherwise specified). The spatial coordinates r, θ, and ϕ are comoving coordinates, meaning that they move with the expansion/contraction of spacetime. For example, an object that has no net force acting on it will have a constant comoving distance from the origin, r, since it is moving only due to the expansion of the universe. The proper distance of that object from the origin at time t is $a(t)r$, which changes in time in accordance with the expansion of spacetime. By solving Einstein's equation using the spatially flat FLRW metric and modeling the contents of the universe as a homogeneous, perfect fluid, we can obtain the Friedmann equations (which bear the name of the previously mentioned Alexander Friedmann):

$$\left(\frac{\dot{a}}{a}\right)^2 = \frac{8\pi G}{3}\rho \tag{1.3}$$

$$\frac{\ddot{a}}{a} = -\frac{4\pi G}{3}(\rho + 3p). \tag{1.4}$$

The dot over a denotes a derivative with respect to time, ρ is the total density of the mass/energy contents of the universe, and p is the fluid pressure of these. Notice that there is no spatial dependence in these equations; this is because we originally assumed isotropy and homogeneity in our universe. These equations are sometimes written in terms of the Hubble parameter, which is the generalization of Hubble's constant for any time: $H \equiv \frac{\dot{a}}{a}$.

The cosmological constant term is usually subsumed as an extra component of the density in the stress-energy tensor as in the following:

$$\rho = \sum_i \rho_i = \rho_{rad} + \rho_m + \rho_\Lambda, \tag{1.5}$$

where the first term is the contribution from radiation from photons and ultrarelativistic neutrinos, the second term from baryonic and dark matter, and the third term from the constant vacuum energy. Another way of expressing the components of mass/energy is

$$1 = \sum_i \Omega_i(t) = \Omega_{rad}(t) + \Omega_m(t) + \Omega_\Lambda(t), \tag{1.6}$$

where $\Omega_i(t)$ for a flat metric is $\frac{\rho_i(t)}{\rho(t)}$. The sum of all the fractions of the total mass/energy in the universe at a given time adds up to 1 for a flat universe. (Sometimes, Ω_i is used to indicate the present-day value of $\Omega_i(t)$ in the literature.) Usually, the equation of state of a perfect fluid component in the stress-energy tensor is modeled as

$$p_i = w_i \rho_i. \tag{1.7}$$

For the cosmological constant model, $w_\Lambda = -1$, and the dark energy density is constant only if this is the case. A universe that contains only the vacuum energy from the cosmological constant is called de Sitter space, named after Willem de Sitter

who found such a solution to Einstein's equation using his cosmological constant term [23]. We usually generalize w_Λ to be w_{DE}, which is not restricted to be -1. A troubling facet of dark energy modeled as a perfect fluid is that it necessarily violates the strong energy condition of general relativity. The energy conditions are meant to loosely dictate what kinds of matter/energy are acceptable and physical. For a perfect fluid, they are as follows:

$$\text{weak energy condition (WEC)}: \ \rho \geq 0, \quad \rho + p \geq 0 \tag{1.8}$$

$$\text{null energy condition (NEC)}: \ \rho + p \geq 0 \tag{1.9}$$

$$\text{strong energy condition (SEC)}: \ \rho + p \geq 0, \quad \rho + 3p \geq 0 \tag{1.10}$$

$$\text{dominant energy condition (DEC)}: \ \rho \geq |p|. \tag{1.11}$$

The cosmological constant model violates the SEC (and not the other energy conditions). We know from observations that our universe during the present epoch is dominated by dark energy, so we can approximate $\rho \approx \rho_{DE}$. From equation (1.4), we see that $\ddot{a}$ (representing acceleration) is positive only if $\rho + 3p$ is negative, i.e., if $w \leq -1/3$. Thus, dark energy as a perfect fluid violates the SEC. (This violation can be shown without assuming $\rho \approx \rho_{DE}$, but we make the assumption for the sake of simplicity.) On the other hand, if $\rho < 0$ and $w = -1$, then $p > 0$, and the SEC is preserved. But then $\ddot{a}$ is not positive, so there is no cosmic acceleration, and the DEC and WEC are violated. However, the most recent observational value of w made by the Nine-Year Wilkinson Microwave Anisotropy Probe (WMAP 9) combining data from WMAP, the CMB, BAO, supernova measurements, and H_0 measurements, is $w = -1.037^{+0.071}_{-0.070}$ at the 95% confidence level [24], assuming a perfect fluid for dark energy, a constant value of w, and a flat universe (which is a good assumption based on observations). So the cosmological constant (CC)

model is in good agreement with observation, and it also agrees with the similar observational value of w when the universe is not assumed to be flat. In fact, the best fit value for w is less than -1, even though all energy conditions are violated for dark energy with $w < -1$ according to equations (1.8) - (1.11). When combined with WMAP polarization and supernova data, the very latest cosmological data, from the Planck satellite, gives $w = -1.13^{+0.013}_{-0.14}$ at the 95% confidence level [25], and the CC model is just barely preserved for this data set. Dark energy with $w < -1$ is known as phantom dark energy, and its density increases over time. Therefore, observations seem to indicate that preserving the SEC and other energy conditions may not be so important. General relativity has not been tested past the scale of our solar system, whereas all the observations that led to this best fit value of w were very far beyond that scale.

Many theoretical dark energy models have been found that are within observational constraints, and many of these models allow w_{DE} to be a function that can change over time. One such form of dynamical dark energy modeled with a scalar field is called quintessence. The equation of motion for the scalar field, which follows from local conservation of mass/energy and momentum, $\nabla_\mu T^\mu_\nu = 0$ (which follows from Einstein's equation), is

$$\nabla_\mu \nabla^\mu \phi + \frac{\partial V}{\partial \phi} = 0, \tag{1.12}$$

where $V(\phi)$ is the scalar field potential. Assuming the scalar field is spatially homogeneous ($\partial^\mu \phi \partial_\mu \phi = \dot{\phi}^2$), The fluid density and pressure of the scalar field are

$$\rho_\phi = \frac{1}{2}\dot{\phi}^2 + V(\phi), \quad p_\phi = \frac{1}{2}\dot{\phi}^2 - V(\phi). \tag{1.13}$$

If $V(\phi) > 0$ and $w_\phi = p_\phi/\rho_\phi < -1$, we see that the kinetic term, $\frac{1}{2}\dot{\phi}^2$, is negative.

Quintessence theories with a negative, non-standard kinetic term are aptly called k-essence theories. Because of the negative kinetic term, the field "rolls up" the potential. Phantom field theories are a bit troublesome since they have "ghosts," or vacuum instabilities. However, these problems can be avoided if they are treated as effective field theories that have momentum cutoffs [26, 27]. And as we have already seen, phantom models seem to be supported by observation, so perhaps such theories will be fleshed out better in the future as we learn more about the nature of dark energy.

1.3 Motivation and Plan of this Work

Cosmologists have come a long way in understanding dark matter and dark energy and their observational constraints, but there are still many unanswered questions. There are still several plausible explanations of these two phenomena.

In chapter two, we explore the possibility of intermediate-mass black holes (IMBHs) comprising all of dark matter. IMBHs typically range in mass from about 10^3 - $10^5 M_\odot$. One aspect of this approach that is beneficial in the interest of efficiency and simplicity is that the introduction of new, unknown particles is not necessary. Black holes are reasonably well understood objects that have theoretical and observational grounding; for example, it is widely accepted from observations that supermassive black holes reside in the center of galaxies. Based on constraints from microlensing and galactic disk stability, both with and without limitations from wide binary surveys, we estimate the total number and entropy of intermediate-mass black holes. Given that the visible universe comprises 10^{11} halos each of mass $\sim 10^{12} M_\odot$, typical core black holes of mean mass $\sim 10^7 M_\odot$ set the dimensionless entropy (S/k) of the universe at a thousand googols (1 googol $= 10^{100}$). One interesting feature of this dark matter candidate is that the entropy

contribution from these IMBHs can exceed that of supermassive black holes in the universe, which are presently the biggest known contributor to the universe's entropy. Identification of all dark matter as black holes allows a dimensionless entropy of the universe up to ten million googols, implying that dark matter can contribute over 99% of entropy. If we hypothesize that, for some dynamical reason, the entropy of the universe is maximized, this favors all dark matter as black holes in the mass regime of $\sim 10^5 M_\odot$.

Chapter three concerns our investigation of dark energy models with non-constant densities. Since such models could possibly describe dark energy, we think it is important to study the dynamics and properties of such models. We study how to distinguish between a cosmological constant and evolving dark energy with equation of state $w(Z)$, where Z is the redshift. Redshift is defined as

$$Z = \frac{\lambda_{observed}}{\lambda_{emitted}} - 1, \tag{1.14}$$

where $\lambda_{observed}$ is the observed wavelength of light from an object in question and $\lambda_{emitted}$ is the wavelength of light emitted. So we detect light that is longer in wavelength (lower in frequency, toward the red end of the electromagnetic spectrum) than that of the original emitted light from an object that is moving away with the expansion of the universe. This effect is somewhat analogous to the Doppler shift. Redshift happens due to the stretching of space, and it happens according to the FLRW metric of spacetime. Redshift due to the expansion of the universe from time t in the past to the present time relates to the scale factor in the following way:

$$Z = \frac{a(t)}{a(t_0)} - 1. \tag{1.15}$$

t_0 is defined to be the present time, and $a(t_0)$, also written as a_0, is usually taken to be 1. We adopt this convention throughout this work unless otherwise specified.

In chapter three, we focus on the value of redshift Z^* at which cosmic acceleration begins, which means that $\ddot{a}(Z^*) = 0$. Four $w(Z)$ are studied, including the well-known CPL model and a new model that has advantages when describing the entire expansion era. If dark energy is represented by a CC model with $w = -1$, Z^* is about 0.7. We discuss the possible implications of a more accurate, model-independent measurement of Z^*.

In 2002, Robert Caldwell [28, 29] explored dark energy models with constant $w_{DE} < -1$, phantom dark energy models. The CC model leads to a constant cosmic acceleration, and thus dark energy provides a constant force on the universe. But for phantom models, the cosmic acceleration is increasing over time. So if the cosmic force due to dark energy gets big enough to overcome the forces holding together bound structures such as galaxies, solar systems, and even the smallest atoms, these structures can be ripped apart in the future. For phantom models, the scale factor a and ρ_{DE} approach infinity at a finite time in the future. Caldwell called such a fate of the universe a "big rip." Chapter four focuses on a particular fate of the universe we have dubbed the "little rip." A little rip model features a dark energy density that increases with time (so that $w_{DE}(a)$ satisfies $w_{DE}(a) < -1$), but w_{DE} approaches -1 asymptotically, and there is no future singularity. We discuss conditions necessary to produce this evolution. Such models can display arbitrarily rapid expansion in the near future, leading to the destruction of all bound structures. We determine observational constraints on two specific parameterizations and calculate the point at which the disintegration of certain bound structures begins. For the same present-day value of w_{DE}, a big rip with constant w_{DE} disintegrates bound structures earlier than a little rip.

Manifestations of little rip models can be via parameterizations of ρ_{DE}, k-essence models, scalar-tensor theories, and models in which dark energy and dark matter

are coupled. We employ all of these in chapter five.

A scalar-tensor theory is simply a theory in which gravity is described by the action of a scalar field along with the usual tensor field of general relativity. One such model we examine in chapter five is given by the action

$$S = \int d^4x\sqrt{-g}\left\{\frac{1}{16\pi G}R - \frac{1}{2}\omega(\phi)\partial_\mu\phi\partial^\mu\phi - V(\phi)\right\}, \tag{1.16}$$

where g is the determinant of the metric, R is the Ricci scalar, and $\omega(\phi)$ and $V(\phi)$ are functions of the field ϕ. $V(\phi)$ is the scalar field potential, and dark energy is represented by ϕ. Without the second and third terms, minimizing the action would result in Einstein's equation for an empty universe, i.e., for a stress-energy tensor $T_{\mu\nu} = 0$. We leave out terms for matter and radiation because we consider this model only when dark energy dominates over other density components, so these terms are negligible.

Usually, different density components are considered independent of each other, but we consider the coupling of dark energy and dark matter, which, given our relative ignorance of the nature of these two, is plausible. Combining the two Friedmann equations, equations (1.3) and (1.4), we can obtain the continuity equation:

$$\dot{\rho} = -3(\rho + p)\frac{\dot{a}}{a} \quad \Rightarrow \quad \frac{d\rho}{da} = -\frac{3}{a}(\rho + p). \tag{1.17}$$

ρ and p can be written as the sum of their components, and if each component is independent of the others, then

$$\sum_i \frac{d\rho_i}{da} = -\sum_i \frac{3}{a}(\rho_i + p_i) \quad \Rightarrow \quad \frac{d\rho_i}{da} = -\frac{3}{a}(\rho_i + p_i) \tag{1.18}$$

for each i. This implies

$$\rho_{rad}(a) = \rho_{rad_0} a^{-4} \quad , \quad \rho_m(a) = \rho_{m_0} a^{-3}, \tag{1.19}$$

where $\rho_{i_0} \equiv \rho_i(a_0)$. The pressure due to a relativistic fluid is $p_{rad} = \frac{\rho_{rad}}{3}$, and cold (non-relativistic) matter is without pressure. From these functional forms for ρ_{rad} and ρ_m, it is clear that radiation dominated the early universe (for small a). As the universe cooled more, matter began to dominate the evolution of the universe, thus $\rho_m(a)$ took over when a became large enough. We study the implications of the coupling between dark matter and dark energy so that the continuity equation for these components are not separable.

Also in chapter five, we derive the conditions for the little rip in terms of the force due to dark energy and present two representative models to illustrate the difference between little rip models and those which are asymptotically de Sitter. We derive conditions on w_{DE} to distinguish between the two types of models. The coupling between dark matter and dark energy with an equation of state that leads to a little rip can alter the evolution, changing the little rip into an asymptotic de Sitter expansion. We give conditions on minimally coupled phantom scalar field models (k-essence models) and on scalar-tensor models that indicate whether or not they correspond to a little rip expansion. We show that, counterintuitively, despite local instability the previously discussed [26, 27], a little rip has an infinite lifetime.

If we assume that the cosmic energy density will remain constant or strictly increase (i.e., monotonically increase) in the future, then the possible fates for the universe can be divided into four categories based on the time asymptotics of the Hubble parameter $H(t)$. Three of the categories, which we have already discussed, are the following: the cosmological constant, for which $H(t) =$ constant; the big

rip, for which $H(t)$ goes to infinity at finite time; and the little rip, for which $H(t)$ goes to infinity as time goes to infinity. In chapter six, we introduce the fourth category, which we call the "pseudo-rip." For a pseudo-rip, $H(t)$ goes to a constant as time goes to infinity, which is an intermediate case between the cosmological constant and the little rip. Because of equation (1.3), "$H(t)$" can be replaced with "ρ" in these four conditions. In chapter six, we provide models that exemplify the pseudo-rip and that fit observational data well. Structures with a binding force at or below a threshold determined by the model's parameters will dissociate. We show that pseudo-rip models for which the density and Hubble parameter increase monotonically can produce an inertial force which does not increase monotonically, but instead peaks at a particular future time and then decreases.

In chapter seven, we conclude and discuss future possible applications and directions in which to continue the research presented in this work.

Chapter 2

Number and Entropy of Black Holes[1]

2.1 Introduction

The identification of dark matter, for which there is compelling evidence from its gravitational effects in galaxies and clusters thereof, is an important outstanding question. Dark matter makes up some eighty percent of matter and a quarter of the energy content of the universe.

Of course, it would be reassuring to identify dark matter by its production in particle colliders and by its detection in terrestrial experiments. On the other hand, the dark matter constituent may equally be, as assumed here, in a completely different and collider-inaccessible mass regime heavier than the Sun.

The observational limits on the occurrence of such multi-solar mass astrophysical objects in the halo have considerably changed recently. There remain microlensing limits [31, 32] on masses below a solar mass and slightly above. There are also respected limits from numerical study [33] of disk stability at ten million solar masses and slightly below.

[1]This chapter is taken from [30].

For the intermediate-mass region, a possible constraint comes from the occurrence of gravitationally bound binary stars at high separation approaching one parsec. Here the situation has changed recently, and the bounds are far more relaxed, possibly non-existent. The first such analysis [34] allowed only some ten percent of halo dark matter for most of the mass range. A more recent analysis [35] permits fifty perecent and cautions that the sample of binaries may be too small to draw any solid conclusions.

In the following, we adopt constraints from microlensing and disk stability but keep an open mind with respect to the wide binaries. We estimate the total number and total entropy of the black holes per halo and hence (simply multiplying by 10^{11}) in the universe, assuming as in [36] that all dark matter can be identified as black holes.

2.2 Number of Black Holes

To estimate number and subsequently entropy of black holes we simplify by taking as possible masses $10^n M_\odot$ with n integer, $1 \leq n \leq 7$. Further, we assume the constraints from wide binaries [35] for different n are independent of each other.

We make our analysis first with binary constraints, denoted simply as "with", then with no binary constraints, denoted as "without". Let f_n be the fraction of the halo dark matter composed of mass $10^n M_\odot$ black holes. The total halo mass is taken to be $10^{12} M_\odot$ whereupon

$$\Sigma_n f_n = 1 \tag{2.1}$$

and the number N_n is

$$N_n = f_n 10^{12-n}. \tag{2.2}$$

The "with" constraints on the f_n are

$$\begin{aligned} 0 &\leq f_1 \leq 0.4 \\ 0 &\leq f_2 \leq 1.0 \\ 0 &\leq f_3 \leq 0.5 \\ 0 &\leq f_{4,5,6} \leq 0.4 \\ 0 &\leq f_7 \leq 0.3. \end{aligned} \tag{2.3}$$

For the "without" constraints, the $f_{1,2,7}$ ranges remain unchanged while the $f_{3,4,5,6}$ are free, namely

$$\begin{aligned} 0 &\leq f_1 \leq 0.4 \\ 0 &\leq f_{2,3,4,5,6} \leq 1.0 \\ 0 &\leq f_7 \leq 0.3. \end{aligned} \tag{2.4}$$

Allowing the f_n to vary by increments $\Delta f_n = 0.1$ for $1 \leq f_n \leq (f_n)_{max}$ we allow the black holes to have ν different mass (or n) values with $1 \leq \nu \leq 7$. For the "with" constraints, we then find numbers of black holes as follows:

ν	# choices	N_{mean}	N_{median}	N_{max}	N_{min}
1	1	1.0×10^{10}	1.0×10^{10}	1.0×10^{10}	1.0×10^{10}
2	24	1.2×10^{10}	8.0×10^{9}	4.6×10^{10}	5.5×10^{9}
3	365	1.4×10^{10}	6.1×10^{9}	4.5×10^{10}	3.4×10^{6}
4	1660	1.6×10^{10}	1.2×10^{10}	4.4×10^{10}	1.2×10^{7}
5	2106	1.6×10^{10}	1.3×10^{10}	4.3×10^{10}	1.1×10^{8}
6	822	1.6×10^{10}	1.2×10^{10}	4.2×10^{10}	1.1×10^{9}
7	83	1.6×10^{10}	1.2×10^{10}	4.1×10^{10}	1.1×10^{10}

Table 2.1: Number of black holes with constraints from wide binaries.

For the "without" case we find:

ν	# choices	N_{mean}	N_{median}	N_{max}	N_{min}
1	5	2.2×10^9	1.0×10^9	1.0×10^{10}	1.0×10^6
2	125	6.1×10^9	9.0×10^8	4.6×10^{10}	7.3×10^5
3	890	1.0×10^{10}	4.0×10^9	4.5×10^{10}	1.6×10^6
4	2340	1.4×10^{10}	1.0×10^{10}	4.4×10^{10}	1.1×10^7
5	2346	1.5×10^{10}	1.2×10^{10}	4.3×10^{10}	1.1×10^8
6	840	1.6×10^{10}	1.2×10^{10}	4.2×10^{10}	1.1×10^9
7	83	1.6×10^{10}	1.2×10^{10}	4.1×10^{10}	1.1×10^{10}

Table 2.2: Number of black holes without constraints from wide binaries.

Study of Tables 1 and 2 reveals a number of things about the putative intermediate-mass black holes which may dominate the matter content. First, the comparison of the tables reveals that the wide binary constraints, as they stand, do not affect the numbers very much. Thus, unless and until a much bigger sample of wide binaries is found (if they exist), the conclusions about numbers of black holes in a halo is insentive to their consideration.

As expected from the defining formula, Eq. (2.2), the number of black holes per halo can range from about a million to a few times ten billion. By sampling distributions of the masses, not just a single mass, Tables 1 and 2 reveal that the most likely number is at the high end, close to ten billion per halo.

Since there are generically 10^{11} halos, this implies a total number of about a billion trillion black holes in the universe.

2.3 Entropy of Black Holes

We can similarly estimate the total entropy of the halo black holes by exploiting the Parker-Bekenstein-Hawking entropy formula [37, 38, 39], which says that for a black hole with mass $M_{BH} = \eta M_\odot$, the entropy is $S_{BH} = 10^{78}\eta^2$.

For the "with" case, this gives the numbers for halo entropy

ν	# choices	S_{mean}	S_{median}	S_{max}	S_{min}
1	1	1.0×10^{92}	1.0×10^{92}	1.0×10^{92}	1.0×10^{92}
2	24	3.0×10^{95}	7.1×10^{93}	3.0×10^{96}	6.4×10^{91}
3	365	7.5×10^{95}	2.2×19^{95}	3.4×10^{96}	1.5×10^{92}
4	1660	1.1×10^{96}	1.0×10^{96}	3.4×10^{96}	1.1×10^{93}
5	2106	1.4×10^{96}	1.2×10^{96}	3.4×10^{96}	1.1×10^{94}
6	822	1.5×10^{96}	1.2×10^{96}	3.3×10^{96}	1.1×10^{95}
7	83	1.6×10^{96}	1.2×10^{96}	3.2×10^{96}	1.1×10^{96}

Table 2.3: Entropy of black holes with constraints from wide binaries.

while for the "without" case we find

ν	# choices	S_{mean}	S_{median}	S_{max}	S_{min}
1	5	2.2×10^{95}	1.0×10^{95}	1.0×10^{96}	1.0×10^{92}
2	125	4.5×10^{95}	8.0×10^{94}	3.7×10^{96}	6.4×10^{91}
3	890	7.7×10^{95}	3.0×10^{95}	3.6×10^{96}	1.5×10^{92}
4	2340	1.1×10^{96}	1.0×10^{96}	3.5×10^{96}	1.1×10^{93}
5	2346	1.3×10^{96}	1.2×10^{96}	3.4×10^{96}	1.1×10^{94}
6	840	1.5×10^{96}	1.2×10^{96}	3.3×10^{96}	1.1×10^{95}
7	83	1.6×10^{96}	1.2×10^{96}	3.2×10^{96}	1.1×10^{96}

Table 2.4: Entropy of black holes without constraints from wide binaries.

Tables 3 and 4 contain much information germane to the central idea that dark matter be identified as black holes.

The biggest known contributor of black holes in a halo is the core supermassive black hole (SMBH). In the Milky Way it is Sag A* and for a typical galaxy a core SMBH has mass $M_{SMBH} \sim 10^7 M_\odot$. Its Parker-Benkenstein-Hawking entropy is therefore about $\sim 10^{92}$.

Multiplying by 10^{11}, the number of halos, shows that these SMBHs contribute about 10^{103}, or a thousand googols, to the entropy of the universe as emphasized in [36].

The conventional wisdom is that the SMBHs are the single dominant contributor to the entropy of the universe, which is therefore about a thousand googols.

From our Tables 3 and 4 we can arrive at a very different conclusion.

2.4 Reconsideration of the Entropy of the Universe

Let us take the viewpoint that the universe, by which we mean the visible universe, is an isolated system in the usual sense of thermodynamics and statistical mechanics. In accord with the usual statistical law of thermodynamics, the entropy of the universe will increase to its maximum attainable value.

The natural unit for the dimensionless entropy of the universe $S/k = \ln \Omega$ is the googol (10^{100}). The supermassive black holes (SMBHs) at galactic cores contribute about a thousand googols.

The holographic bound [40] on information or entropy contained in a three-volume is that it be not above the surface area as measured in Planck units $(10^{-33} cm^2)$. If we take the visible universe to be a sphere of radius $3 \times 10^{10} ly \sim 3 \times 10^{18} cm$, the maximum entropy is $\sim 10^{124}$ or a trillion trillion googols. This would be the entropy if the universe were one black hole of mass $10^{23} M_{\odot}$.

The numbers in Tables 3 and 4 suggest that the entropy contribution from dark matter can exceed that of the SMBHs by orders of magnitude. Taking the view that increasing total entropy plays a dominant role in cosmological evolution strongly favors the formation of black holes in the $10^5 M_{\odot}$ mass range and the view that they constitute all dark matter.

We are more confident about the present status of dark matter than of its detailed history but, of course, an interesting and legitimate question is: how did the black holes originate? One possible formation is as remnants of Population-III (henceforth Pop-III) stars formed at a redshift $Z \sim 25$. These Pop-III stars are necessary to explain the metallicity of Pop-I and Pop-II stars that formed later. Such Pop-III stars are not well understood but we expect they can be very massive,

$10^5 M_\odot$, to live for a short time, less that a million years, then explode leaving black holes which have a total mass that is a significant fraction of the original star's mass. Nevertheless, it is very unlikely [41] that a sufficient number of Pop-III stars can form to make all dark matter. Thus, the IMBHs may have formed in the early universe as primordial black holes.[2]

The first item of business is therefore to confirm that there are millions of large black holes in our halo and in others.

The ESA Gaia project is planned to survey billions of stars in our galaxy, the Milky Way, and should enable obtaining a large sample of gravitationally bound wide binaries which can be analyzed for evidence of black holes perturbing them.

The goal of the SuperMACHO project is to identify the objects which produced existing microlensing events and should allow the observation of higher longevity microlensing signals corresponding to the mass ranges suggested for the dark matter black holes.

Finally, if we truncate to $n \leq 5$, since Pop-III stars or IMBHs with higher masses seem unlikely [41], then the typical number of IMBHs per halo is $\sim 10^{10}$, giving about one million googols for the entropy of the universe. The majority of entropy may be concentrated in a tiny fraction of the total number of black holes as can be seen by studying examples, e.g., $f_2 = f_5 = 0.5$.

The key motivation for our believing this interpretation of dark matter, as opposed to an interpretation involving microscopic particles, comes from consideration of the entropy of the universe. The SMBHs at galactic cores contribute about a thousand googols to the overall dimensionless entropy. As seen in the present article, dark matter in the form of black holes can contribute as much as a million

[2]Note that the constraints in [21] apply at the recombination era and subsequent black hole mergers can occur.

googols and thus make up over 99% of the cosmic entropy, which is sufficient reason, if we adopt that the universe is an isolated system to which the second law of thermodynamics is applicable, for taking it seriously.

Hopefully future observations will be able to identify dark matter as black holes.

Chapter 3

Seeking Evolution of Dark Energy[1]

3.1 Introduction

The interface between astrophysics and particle physics has never been stronger than now because our knowledge of gravity comes in large part from observational astronomy and cosmology. At particle colliders, seeking the constituent of dark matter is an important target of opportunity.

Dark energy is widely regarded as the most important issue in all of physics and astronomy. Other than the cosmological constant (CC) model, and the very interesting, if not yet fully satisfying, usage of string theory, there is no compelling theory. So we are motivated to pursue a purely phenomenological approach to attempt to make progress towards the understanding of dark energy.

The discovery of cosmic acceleration [13, 12] in 1998 has revolutionized theoretical cosmology. The simplest theoretical interpretation is as a CC with constant density and equation of state (EoS) $w \equiv -1$. We shall refer to alternatives to the CC model, with $w(Z)$ redshift-dependent, as evolutionary dark energy.

[1]This chapter is taken from [42].

The equations which govern cosmic history, which assume Einstein's equations, isotropy, homogeneity (FLRW metric [2, 3, 4, 5]), and flatness as expected from inflation, are (with $c = 1$):

$$H(t)^2 = \left(\frac{\dot{a}}{a}\right)^2 = \left(\frac{8\pi G}{3}\right)\rho \tag{3.1}$$

and

$$\left(\frac{\ddot{a}}{a}\right) = -\frac{4\pi G}{3}(\rho + 3p), \tag{3.2}$$

together with the continuity equation:

$$a\frac{d\rho}{da} = -3(\rho + p). \tag{3.3}$$

In these equations, p is pressure and ρ is the density with components $\rho = \rho_\Lambda + \rho_m + \rho_\gamma$. Although, for small redshifts, the radiation term is by far the smallest, we still include it.

Using Eq. (3.2), the CC model with $w \equiv -1$, and the WMAP7 values[2]

$$\Omega_\Lambda(t_0) = 0.725 \pm 0.016 \quad \text{and} \quad \Omega_m(t_0) = 0.274 \pm 0.013, \tag{3.4}$$

we find that [44]

$$Z^* = \left(\frac{2\Omega_\Lambda(t_0)}{\Omega_m(t_0)}\right)^{\frac{1}{3}} - 1 \;=\; 0.743 \pm 0.030. \tag{3.5}$$

With evolution, Eq. (3.5) is modified. It is worth mentioning that Z^* is a constant of Nature, like Hubble's constant, which can in principle be measured

[2]Note that we use the WMAP7 [43] value for $\Omega_m(t_0)$, unless explicitly stated otherwise. We use $\Omega_\gamma(t_0) = 5 \times 10^{-5}$.

precisely, without reference to any theoretical model. We shall introduce various evolutionary models, including the very popular CPL model [45, 46] $w^{(CPL)}(Z)$ and a new proposal $w^{(new)}(Z)$ that is more physically motivated with respect to the whole expansion history[3]. We present figures which make predictions for Z^*, and we suggest slowly varying criteria which support the use of $w^{(new)}(Z)$ over $w^{(CPL)}(Z)$.

3.2 Evolutionary Dark Energy Models

When we consider dark energy models, we must specify an equation of state $w(Z)$. There is an infinite number of choices for $w(Z)$: our objective in the present article is to suggest a sensible choice for the functional form of $w(Z)$, which can be valid for the entire extent of the present expansion era. Since there exists no compelling evolutionary theory, we choose to consider models for $w(Z)$ each containing two free parameters, which we designate as w_0 and w_1, each ornamented by a superscript which denotes the model. To add more parameters would be premature. The first three are already in the literature, while the fourth is, to our knowledge, new.

(i) Linear model (lin)

The evolutionary equation of state (EEoS) is:

$$w^{(lin)}(Z) = w_0^{(lin)} + w_1^{(lin)} Z \tag{3.6}$$

(ii) Chevallier-Polarski-Linder model [45, 46] (CPL)

[3]References [45, 46] do, however, specify that the CPL model is to be used only for $0 \leq Z \lesssim 2$.

The EEoS for CPL is:

$$w^{(CPL)}(Z) = w_0^{(CPL)} + w_1^{(CPL)} \frac{Z}{1+Z} \tag{3.7}$$

(iii) Shafieloo-Sahni-Starobinsky model [47] (SSS)

The SSS version of the EEoS is:

$$w^{(SSS)}(Z) = -\frac{1 + \tanh[(Z - w_0^{(SSS)}) w_1^{(SSS)}]}{2} \tag{3.8}$$

(iv) New proposal (new)

Here we consider, as a novel EEoS, a simple modification of the CPL EEoS:

$$w^{(new)}(Z) = w_0^{(new)} + w_1^{(new)} \frac{Z}{2+Z} \tag{3.9}$$

3.3 Analysis of the Models

We begin with the model where the EEoS is linear in redshift, $w^{(lin)}(Z)$. In Fig. 3.1 are shown $w_0^{(lin)} - w_1^{(lin)}$ curves for Z^* in the range $0.4 \leq Z^* \leq 0.9$. Several interesting features of Fig. 3.1 deserve discussion. First, the dot at (0, -1) confirms $Z^* = 0.743 \pm 0.030$ for the CC model. If Z^* is measured to be $Z^* > 0.75$, it is necessary that $w_1^{(lin)} < 0$. If Z^* is meaured to be $Z^* > 0.831$, we find that $w_0^{(lin)} > -1$. As Z^* increases, the requisite $w^{(lin)}(Z)$ becomes more and more distinct from the CC model. In Fig. 3.1, we note that for any measured value of Z^*, there are two possible values of $w_0^{(lin)}$ for each value of $w_1^{(lin)}$.

The EEoS for $w^{(lin)}(Z)$ possesses singular behavior for $Z \to \infty$ because $w^{(lin)}(Z) \to \pm\infty$ for $w_1^{(lin)}$ being positive or negative, respectively.

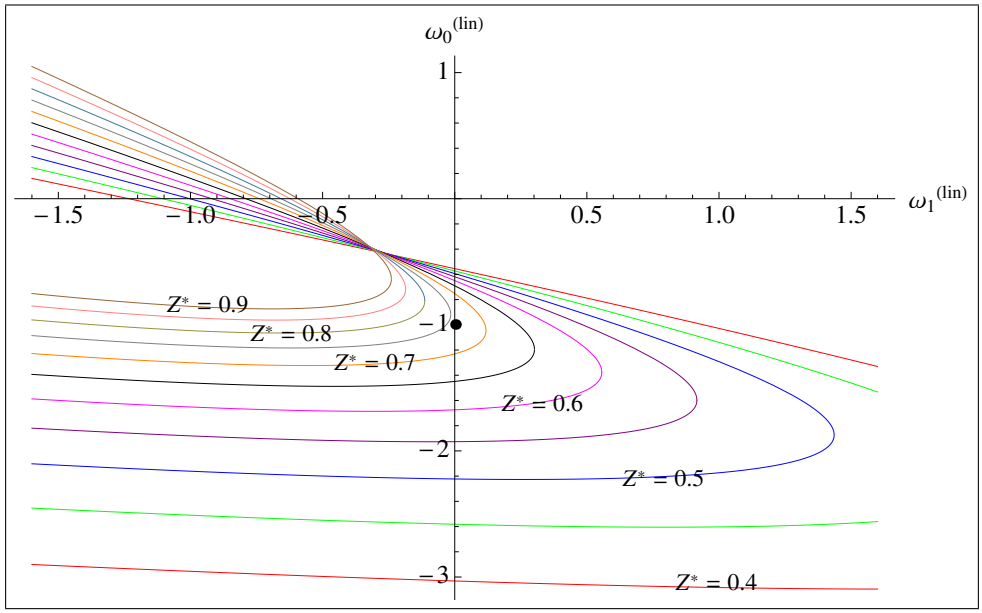

Figure 3.1: $w_0^{(lin)}$ is plotted against $w_1^{(lin)}$ for $0.4 \leq Z^* \leq 0.9$ in increments of 0.05. The dot at (0,-1) represents the CC model. Here we use $\Omega_m(t_0) = 0.275$, which is consistent with the result of [48] for the best fit for this model.

The reader will remark the confluence of the Z^*-orbits in Fig. 3.1, which is an artifact of the restriction to $0.4 \leq Z^* \leq 0.9$. For values of Z^* near to but outside this range, the confluence desists. A similar phenomenon appears in later plots.

We next discuss the model $w^{(CPL)}(Z)$ [45, 46] in which the EEoS is linear in $(1-a)$, where a is the scale factor. In Fig. 3.2 are shown $w_0^{(CPL)} - w_1^{(CPL)}$ curves for Z^* in the range $0.6 \leq Z^* \leq 1.0$. There are several features of Fig. 3.2 to note. The dot at (0, -1) confirms $Z^* = 0.8$, which is the resulting Z^* value from Eq.(3.5) when the value $\Omega_m(t_0) = 0.255$ is used, as determined by [47] as the best fit value for the CPL model. If Z^* is measured to be $Z^* > 0.810$, we find that $w_1^{(CPL)} < 0$. As Z^* increases, the necessary $w^{(CPL)}(Z)$ becomes more and more distinct from the CC model. In Fig. 3.2, we see that for any measured value of Z^*, there are two possible values of $w_0^{(CPL)}$ for each value of $w_1^{(CPL)}$.

Now we examine Fig. 3.3 for the SSS model. We see that for a certain range of $Z^* > 0.8$, which includes the best fit value of Z^* which we discuss later, both

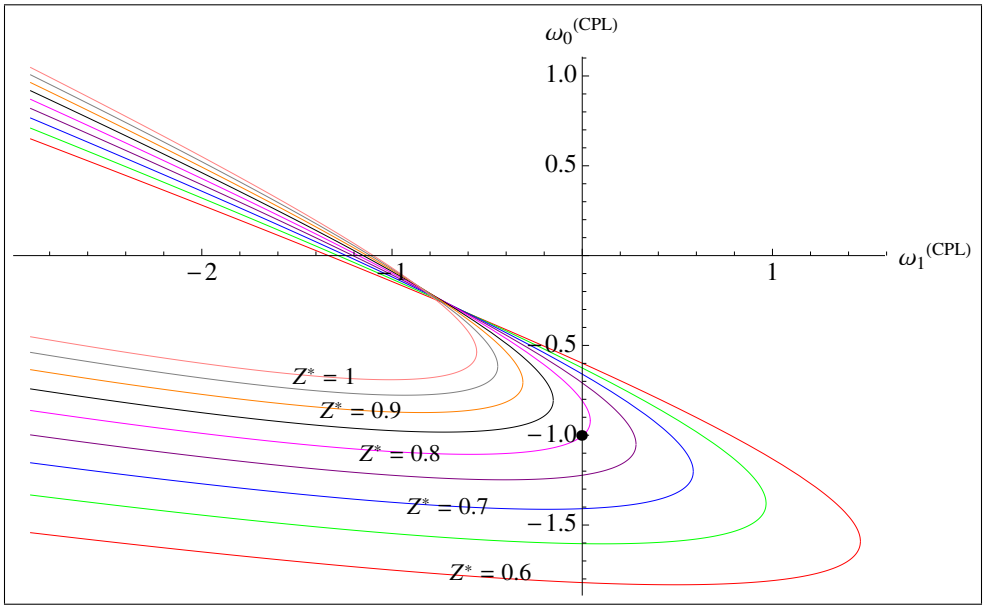

Figure 3.2: $w_0^{(CPL)}$ is plotted against $w_1^{(CPL)}$ for $0.6 \leq Z^* \leq 1.0$ in increments of 0.05. The dot at (0,-1) represents the CC model. We use $\Omega_m(t_0) = 0.255$, which is consistent with the analysis in [47] for the best fit for this model.

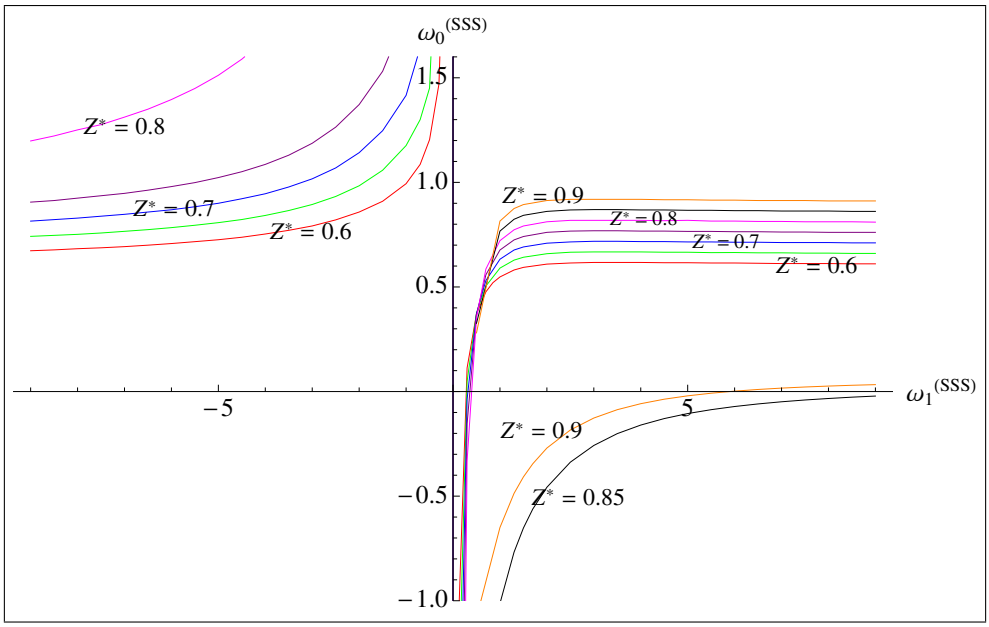

Figure 3.3: $w_0^{(SSS)}$ is plotted against $w_1^{(SSS)}$ for $0.6 \leq Z^* \leq 0.9$ in increments of 0.05. We use $\Omega_m(t_0) = 0.255$, which is consistent with the analysis in [47] for the best fit for this model.

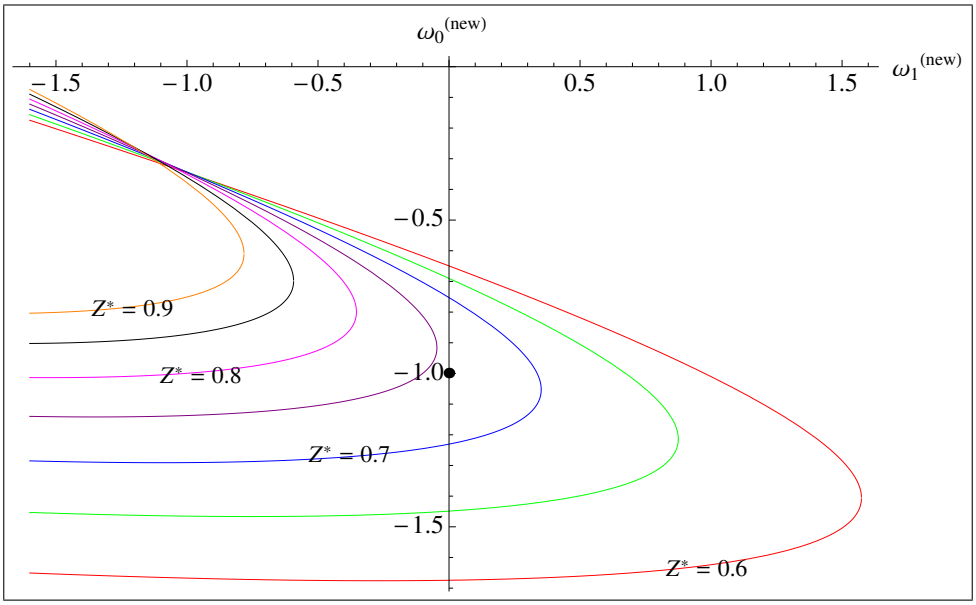

Figure 3.4: $w_0^{(new)}$ is plotted against $w_1^{(new)}$ for $0.6 \leq Z^* \leq 0.9$ in increments of 0.05. The dot at (0,-1) represents the CC model. We use $\Omega_m(t_0) = 0.275$.

$w_1^{(SSS)}$ and $w_0^{(SSS)}$ must be greater than zero. Note also the degeneracy in $w_0^{(SSS)}$ for $Z^* = 0.85, 0.9$.

Fig. 3.4 displays the new model. Once again we see that the CC model has $Z^* = 0.743$. For $Z^* \geq 0.81$, $w_0^{(new)} > -1.0$. We note that for $Z^* > 0.75$, $w_1^{(new)}$ must be negative.

In Fig. 3.5, we show $w^{(lin)}(Z)$, $w^{(CPL)}(Z)$, and $w^{(SSS)}(Z)$ as a function of Z (including the future, $-1 \leq Z < 0$) using the best-fit parameters of [48] for $w^{(lin)}(Z)$ and those of [47] for the other 2 models. $w^{(new)}(Z)$ is also plotted using the choice of $w_0^{(new)} = -1$ and $w_1^{(new)} = 0.1$.

Unlike the CC model, where the future of the universe is infinite exponential expansion, the best fit for $w^{(lin)}(Z)$ necessarily leads to a big rip, at a finite time in the future. The EEoS for $w^{(CPL)}(Z)$ possesses singular behavior for $Z \to -1$ because $w^{(CPL)}(Z) \to \pm\infty$ for $w_1^{(CPL)}$ being negative or positive, respectively. For the SSS model, $w^{(SSS)}(Z)$ varies in the range $0 > w^{(SSS)}(Z) > -1$.

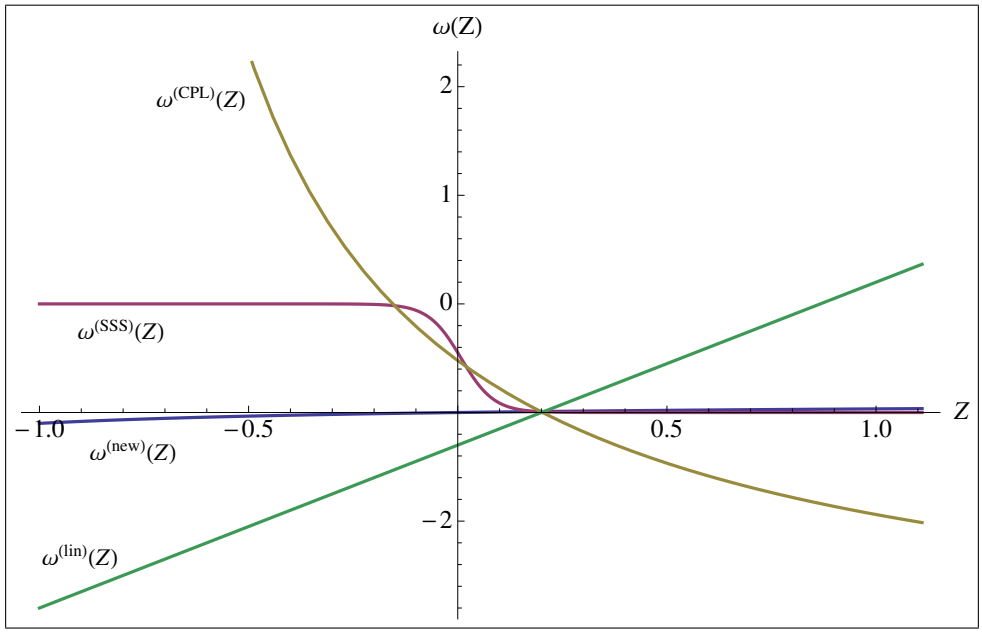

Figure 3.5: $w(Z)$ for all the models is plotted against Z from the highest Z^* value to $Z = -1$ (when the scale factor a is infinite). The horizontal axis at $w(Z) = -1$ is the line representing the CC model. We use $w_0^{(lin)} = -1.3$, $w_1^{(lin)} = 1.5$, and $Z^* = 0.4067$ (from the best fit for this model given in [48]). We use $w_0^{(CPL)} = -0.522$, $w_1^{(CPL)} = -2.835$, and $Z^* = 1.11$ for the CPL model and $w_0^{(SSS)} = 0.008$, $w_1^{(SSS)} = 12.8$, and $Z^* = 0.855$ for the SSS model (both from the respective best fits given in [47]). $w^{(new)}(Z)$ is plotted using $w_0^{(new)} = -1$ and $w_1^{(new)} = 0.1$, which gives $Z^* = 0.729$.

As for our fourth and last model $w^{(new)}(Z)$, from Eq.(3.9), we note that this choice has the advantage that for all Z this EEoS lies between $(w_0^{(new)} - w_1^{(new)})$ and $(w_0^{(new)} + w_1^{(new)})$. This is illustrated in Fig 3.5 where, for the choices $w_0^{(new)} = -1.0$ and $w_1^{(new)} = +0.1$, the EEoS falls smoothly from -0.9 at the big bang to -1.1 at the big rip.

3.4 Slowly Varying Criteria

We now discuss which $w(Z)$ for dark energy is the best for observers to employ. Regretfully, there is no theoretical guidance about evolution. Nevertheless, we here propose slowly varying criteria which is based purely on grounds of aesthetics and, especially, conservatism. All the present data are consistent with the CC model $w^{(CC)} \equiv -1$. We choose to remain proximate to it, as supported by [49, 50]. One consideration is that we prefer any global $w(Z)$ to have analytic, non-singular behavior for $Z \to -1$ and $Z \to \infty$. Finally, we propose to impose the inequality representing conservatism,

$$|w(Z) + 1| \ll 1 \quad \text{for all} \quad -1 \leq Z < \infty. \tag{3.10}$$

Next, we consider application of our slow variation criteria to the four specific models we have discussed in tbe present article. For this task, Fig. 3.5 will be used. To be fair to their inventors, these EEoS were intended to apply for only a limited range of redshift.

(i) Linear model

By studying the EEoS in Eq. (3.6), we notice that for $Z \to +\infty$, $w^{(lin)}(Z)$ approaches $\pm\infty$ depending on the sign of $w_1^{(lin)}$. Also, $w^{(lin)}(Z)$ violates the criterion of Eq.

(3.10). We conclude that this linear model is disfavored according to our slow variation criteria.

(ii) CPL model

By examining the EEoS in Eq. (3.7), we note that as $Z \to -1$, $w^{(CPL)}(Z) \to \mp\infty$ for a ($\pm$) sign for $w_1^{(CPL)}$. Therefore, according to our criteria, this model is disfavored.

(iii) SSS model

Looking at Eq. (3.8), we see that $w^{(SSS)}(Z)$ varies from 0 to -1 for the best fit given in [47], so it is non-singular. By this token, however, it does not satisfy Eq. (3.10). This model, then, is also disfavored by our criteria. It should be noted, though, that [47] studied this EEoS as a toy model to illustrate the importance of an EEoS that fits data well for small and large positive Z.

(iv) New model

This model is non-singular for all $-1 \leq Z < \infty$ because $[Z/(2+Z)]$ varies smoothly from -1 to $+1$, as can be seen from examining Eq. (3.9). It also satisfies Eq. (3.10) if we choose appropriate values for $w_0^{(new)}$ and $w_0^{(new)}$.

3.5 Discussion and Conclusions

The outstanding observational question about dark energy is whether it is a CC model with $w(Z) \equiv -1$ or an evolutionary model with a non-trivial EEoS. The model-independent observational measurement of Z^* is very useful for making this distinction.

The theoretical prediction of Z^* is, however, dependent on the EoS that is assumed. The value for the CC model using the WMAP7 values of $\Omega_m(t_0)$ and $\Omega_\Lambda(t_0)$

is $Z^* = 0.743 \pm 0.030$. As the data become even more precise, the error on Z^* will diminish, making it observationally easier to detect deviation, if any, from the CC model.

In the four EEoS models listed earlier, the possible values of Z^* for different values of the parameters w_0 and w_1 can be read off from our plots. These plots show that degeneracies appear. For a given Z^* and a specific type of EEoS, there is an allowed curve in the w_1-w_0 plane. For all $0.4 \leq Z^* \leq 1.0$, there exist disallowed regions in the w_1-w_0 plane.

To go further, we have to give criteria for selecting one EEoS. The most popular choice in the last few years has been the CPL model [45, 46] because it approximates the linear model at low redshift. Also, it has a simple interpretation in terms of the scale factor:

$$w^{(CPL)}(Z) = w_0^{(CPL)} + w_1^{(CPL)}(1 - a(Z)) \tag{3.11}$$

However, as $a(Z) \to \infty$ ($Z \to -1$), the CPL model diverges. Of course, the authors of [45, 46] intended their model to be applicable only for a limited range of Z. However, it seems preferable for $w(Z)$ to cover the entire range of cosmic history, both the past and future.

Our novel EEoS also approximates the linear model at low redshift. It has, like the CPL model, a straightforward physical interpretation in terms of the scale factor:

$$w^{(new)}(Z) = w_0^{(new)} + w_1^{(new)} \left(\frac{1 - a(Z)}{1 + a(Z)} \right) \tag{3.12}$$

We think one advantage of this new model over the CPL model is that it is non-singular for $-1 \leq Z < \infty$. A second advantage is that it can satisfy the slow variation criterion of Eq. (3.10).

In conclusion, the choice of an evolutionary alternative to the CC model depends theoretically on constraining the EEoS, and we have proposed a new EEoS which not only has a simple physical interpretation but also is well-behaved for all possible redshifts. The model-independent extraction of Z^* from observational data is a familiar process [51]. A more accurate model-independent estimate of Z^* by global fits to all relevant data is worthwhile. It is an interesting issue how the present considerations of evolutionary dark energy are related to the possible occurrence of a big rip. This requires ultra-negative pressures of dark energy, so it is interesting that situations involving phantom energy have appeared in the context of extra spatial dimensions in string theory [52].

It has been argued [53] that dark energy effects can be detected only by studying physical systems as large as galaxies. Thus, it is unlikely that any terrestrial experiment can be sensitive to dark energy.

Understanding dark energy may, or may not (in the CC model), require a gravitational theory more complete than general relativity, which has been accurately confirmed [54] only at the scale of the solar system, say $\sim 10^{12}$ meters, while dark energy operates above the galactic size, say $\sim 10^{20}$ meters. Thus, it is likely, even probable, that study of dark energy will inform us, in the near future, how to go beyond Einstein, which is the most important direction both for particle physics and astrophysics.

Chapter 4

The Little Rip[1]

4.1 Introduction

Observations indicate that roughly 70% of the energy density in the universe is in the form of an exotic, negative-pressure component, dubbed dark energy [56, 57]. (See Ref. [58] for a recent review.) If ρ_{DE} and p_{DE} are the density and pressure, respectively, of the dark energy, then the dark energy can be characterized by the equation-of-state parameter w_{DE}, defined by

$$w_{DE} = p_{DE}/\rho_{DE}. \tag{4.1}$$

It was first noted by Caldwell [28] that observational data do not rule out the possibility that $w_{DE} < -1$. Such "phantom" dark energy models have several peculiar properties. The density of the dark energy *increases* with increasing scale factor, and both the scale factor and the phantom energy density can become infinite at a finite t, a condition known as the "big rip" [28, 29, 59, 60]. It has even been suggested that the finite lifetime for the universe in these models may provide an

[1]This chapter is taken from [55].

explanation for the apparent coincidence between the current values of the matter density and the dark energy density [61].

While $w(a) < -1$ as a extends into the future is a necessary condition for a future singularity, it is not sufficient. In particular, if w approaches -1 sufficiently rapidly, then it is possible to have a model in which ρ_{DE} increases with time, but in which there is no future singularity. Conditions which produce such an evolution (specified in terms of p_{DE} as a function of ρ_{DE}) were explored in Refs. [62, 63, 64].

In this paper, we examine such models in more detail. In particular, we will extend the parameter space discussed in Refs. [62, 63, 64] in both directions, showing that there are nonsingular models in which ρ_{DE} increases more rapidly than the nonsingular models discussed in those references, and, conversely, that there are singular models with ρ_{DE} increasing less rapidly than the singular models discussed in Refs. [62, 63, 64]. Models without a future singularity in which ρ_{DE} increases with time will nonetheless eventually lead to a dissolution of bound structures at some point in the future, a process we have dubbed the "little rip." We discuss the time scales over which this process occurs. Finally, we consider observational constraints on these models.

In the next section, we examine the conditions necessary for a future singularity in models with $w < -1$. In Secs. III and IV, specific little rip models and disintegration of bound systems are studied. Finally, in Sec. V, there is discussion.

4.2 The Conditions for a Future Singularity

We limit our discussion to a spatially flat universe, for which the Friedmann equation is

$$\left(\frac{\dot{a}}{a}\right)^2 = \frac{\rho}{3}, \tag{4.2}$$

where ρ is the total density, a is the scale factor, the dot will always denote a time derivative, and we take $\hbar = c = 8\pi G = 1$ throughout. We will examine the future evolution of our universe from the point at which the pressure and density are dominated by the dark energy, so we can assume $\rho = \rho_{DE}$ and $p = p_{DE}$, and for simplicity we will drop the DE subscript. Then the dark energy density evolves as

$$\dot{\rho} = -3\left(\frac{\dot{a}}{a}\right)(\rho + p). \tag{4.3}$$

The simplest way to achieve $w < -1$ is to take a scalar field Lagrangian with a negative kinetic term, and the conditions necessary for a future singularity in such models have been explored in some detail [65, 66, 67, 68]. Here, however, we explore the more general question of the conditions under which a dark energy density that increases with time can avoid a future singularity, and the consequences of such models.

One can explore this question from a variety of starting points, by specifying, for example, the scale factor a as a function of the time t (an approach taken, for example, in Refs. [69, 70, 71, 72]). Alternately one can specify the pressure p as a function of the density ρ, as in Refs. [62, 63, 64]. Note that this is equivalent to specifying the equation-of-state parameter w as a function of ρ, since $w = p/\rho$. Finally, one can specify the density ρ as a function of the scale factor a. Since we are interested specifically in nonsingular models for which ρ increases with a, we shall adopt this last approach, but we will briefly examine the other two starting points. Of course, given any one of these three functions, the other two can be derived uniquely, but not always in a useful form.

For example, suppose that we specify $a(t)$. In order to avoid a big rip, it is

sufficient that $a(t)$ simply be a nonsingular function for all t. Writing

$$a = e^{f(t)}, \tag{4.4}$$

where $f(t)$ is a nonsingular function, the density is given by equation (4.2) as $\rho = 3(\dot{a}/a)^2 = 3\dot{f}^2$, and the condition that ρ be an increasing function of a is simply $d\rho/da = (6/\dot{a})\dot{f}\ddot{f} > 0$, which is satisfied as long as

$$\ddot{f} > 0. \tag{4.5}$$

Thus, all little rip models are described by an equation of the form (4.4), with nonsingular f satisfying equation (4.5).

Now consider the approach of Refs. [62, 63, 64], who expressed the pressure as a function of the density in the form

$$p = -\rho - f(\rho), \tag{4.6}$$

where $f(\rho) > 0$ ensures that the ρ increases with scale factor. In order to determine the existence of a future singularity, one can integrate equation (4.3) to obtain [62, 63]

$$a = a_0 \exp\left(\int \frac{d\rho}{3f(\rho)}\right), \tag{4.7}$$

and equation (4.2) then gives [62, 63]

$$t = \int \frac{d\rho}{\sqrt{3\rho} f(\rho)}. \tag{4.8}$$

The condition for a big rip singularity is that the integral in equation (4.8) converges. Taking a power law for $f(\rho)$, namely

$$f(\rho) = A\rho^{\alpha}, \tag{4.9}$$

we see that a future singularity can be avoided for $\alpha \leq 1/2$ [62, 63, 64]. We examine this boundary in more detail below, noting that one can have $f(\rho)$ increase more rapidly than $\rho^{1/2}$ without a future singularity.

Now consider the third possibility: specifying the density ρ as an increasing function of scale factor a. We will seek upper and lower bounds on the growth rate of $\rho(a)$ that can be used to determine whether or not a big rip singularity is produced. Defining $x \equiv \ln a$, we can rewrite equation (4.2) as

$$t = \int \sqrt{\frac{3}{\rho(x)}} dx, \tag{4.10}$$

and the condition for avoiding a future big rip singularity is

$$\int_{x_0}^{\infty} \frac{1}{\sqrt{\rho(x)}} dx \to \infty. \tag{4.11}$$

The case $p = -\rho - A\rho^{1/2}$ from Refs. [62, 63, 64] corresponds to

$$\frac{\rho}{\rho_0} = \left(\frac{3A}{2\sqrt{\rho_0}} \ln(a/a_0) + 1 \right)^2, \tag{4.12}$$

where $w \leq -1$ requires $A \geq 0$, and we take $\rho = \rho_0$ and $a = a_0$ at a fixed time t_0. Expressing this density as a function of time rather than scale factor gives a much simpler expression:

$$\frac{\rho}{\rho_0} = e^{\sqrt{3}A(t-t_0)}. \tag{4.13}$$

The equation-of-state parameter w corresponding to equation (4.12) can be derived

from the relation $(a/\rho)(d\rho/da) = -3(1+w)$:

$$w = -1 - \frac{1}{\frac{3}{2}\ln(\frac{a}{a_0}) + \frac{\sqrt{\rho_0}}{A}}, \tag{4.14}$$

and the corresponding expansion law is

$$\frac{a}{a_0} = e^{(2\sqrt{\rho_0}/3A)[e^{(\sqrt{3}A/2)(t-t_0)}-1]}. \tag{4.15}$$

However, we can find $\rho(a)$ for which ρ increases more rapidly with a, but for which equation (4.11) is still satisfied. For example, writing $\rho^{1/2} \sim (\ln a)(\ln\ln a)$ as $a \to \infty$ satisfies equation (4.11). An example of such a ρ, with a free parameter B, is

$$\frac{\rho}{\rho_0} = N\left(\frac{a}{a_0}, B\right)\frac{(1+\ln(\frac{a}{a_0}+B))^2}{(1+\ln(1+B))^2}\frac{(\ln(1+\ln(\frac{a}{a_0}+B)))^2}{(\ln(1+\ln(1+B)))^2}, \tag{4.16}$$

where the choice

$$N\left(\frac{a}{a_0}, B\right) = \frac{(\frac{a}{a_0}+B)^2}{(1+B)^2(\frac{a}{a_0})^2} \tag{4.17}$$

leads to a real, nonnegative ρ and an analytic form for the behavior of $a(t)$:

$$\frac{a}{a_0} = e^{(e^{\ln(1+\ln(1+B))e\left[\frac{\sqrt{\rho_0/3}(t-t_0)}{(1+B)(1+\ln(1+B))\ln(1+\ln(1+B))}\right]}-1)} - B. \tag{4.18}$$

This argument can be extended further. In general, if we denote $\ln_j(x) \equiv \ln\ln\ln....\ln(x)$, where the logarithm on the right-hand side is iterated j times, then any function of the form

$$\rho \sim (\ln a)^2(\ln_2 a)^2(\ln_3 a)^2...(\ln_m a)^2 \tag{4.19}$$

satisfies equation (4.11) as $a \to \infty$ and avoids a big rip singularity. A density

increasing as in equation (4.19) leads to an expansion law of the form

$$a \sim \exp(\exp(\exp ...(\exp(t))...)), \tag{4.20}$$

where there are $m + 1$ exponentials. We have omitted the constants in equations (4.19) and (4.20) for the sake of clarity. Equation (4.20), while growing extraordinarily rapidly, is manifestly nonsingular. While an expansion law of this sort might seem absurd, it is probably less so than a big rip expansion law, and in any case our goal is to try to determine the boundary between little rip and big rip evolution for $\rho(a)$. In this spirit, consider the slowest growing power-law modification to equation (4.19):

$$\rho \sim (\ln a)^2 (\ln_2 a)^2 (\ln_3 a)^2 ... (\ln_m a)^{2+\epsilon}, \tag{4.21}$$

where $\epsilon > 0$ is a constant. No matter how small ϵ is, and despite the fact that it modifies an extraordinarily slowly growing nested logarithm function, the growth law in equation (4.21) leads to a future big rip singularity.

Note that the bounds specified by equations (4.19) and (4.21) are not sharp; we can always find forms for $\rho(a)$ that interpolate between these two behaviors and produce either a little rip or a big rip. However, as we take m to be arbitrarily large, nearly any function of interest will increase more rapidly than equation (4.19) or more slowly than equation (4.21), allowing us a practical, if not a rigorously sharp, bound. This lack of a sharp bound is due to the fact that there is no bound on the fastest growing function $a(t)$ which is nonsingular at finite t.

If one is willing to place other restrictions on the form of $\rho(a)$, then more stringent bounds apply. Barrow [73] demonstrated that if $\rho + 3p$ is a rational function of a and t, and $a(t)$ is nonsingular at finite t, then $a(t)$ can grow no more rapidly

than the double exponential of a polynomial in t. Our equation (4.19) violates this condition because of the logarithmic functions.

4.3 Constraining Little Rip Models

Here we shall examine in more detail the two specific little rip models given by equations (4.12) and (4.16), which we will call model 1 and model 2, respectively. Note that we do *not* make use of equations (4.15) and (4.18) here, as these are valid only when the matter density can be neglected in comparison to the dark energy density. Model 1 is characterized by a single free parameter A, and the scale factor behaves asymptotically as a double exponential in t, as in equation (4.15):

$$a(t) \overset{t\to+\infty}{\longrightarrow} e^{e^{t}} \tag{4.22}$$

The parameter A is chosen to make a best fit to the latest supernova data from the Supernova Cosmology Project [74], and has the best-fit value $A = 3.46\times10^{-3}\mathrm{Gyr}^{-1}$, while a 95% C.L. fit can be found for the range $-2.74 \times 10^{-3}\mathrm{Gyr}^{-1} \leq A \leq 9.67 \times 10^{-3}\mathrm{Gyr}^{-1}$.

Model 2 is characterized by the free parameter B and has a scale factor that behaves asymptotically as a triple exponential in t, as in equation (4.18):

$$a(t) \overset{t\to+\infty}{\longrightarrow} e^{e^{e^{t}}} \tag{4.23}$$

The parameter B is chosen to make a best fit to [74] as well, and it has the value $B = 1.23$. The confidence interval for B at the 95% C.L. is $1.12 \leq B \leq 1.34$. In fitting both models, $\Omega_{m_0} = 0.274$, $\Omega_{x_0} = 1 - \Omega_{m_0}$, and $H_0 = 70.1$ km s^{-1} Mpc^{-1}, which are consistent with the best-fit ranges for these values given by WMAP [75].

The resultant Hubble and residual ΛCDM ($w = -1$) plots of distance modulus μ versus redshift z for both models are displayed in Fig. 1.

Not surprisingly, the best-fit models closely resemble the ΛCDM model, which is known to be an excellent fit to the data [50]. To see this more clearly, note that our models will resemble a cosmological constant at low redshift as long as $\rho(a) \sim constant$ for $a \sim a_0$. For model 1, this condition is satisfied when $A/\sqrt{\rho_0} \ll 1$ in equation (4.12), while for model 2, we require $B \simeq 1.39$ in equation (4.16). To see that B should be close to this value, one should expand equation (4.16) around $a = a_0$. The zeroth-order term is ρ_0, and the coefficient for the first-order term is 0 when $B = 1.39$. A comparison with our best-fit values indicates that these conditions are, indeed, satisfied. Furthermore, in the limit where these conditions are satisfied, these little rip models closely resemble, at low redshift, big rip models close to ΛCDM, i.e., models with constant $w < -1$ and $|1 + w| \ll 1$. To see this, recall that constant-w big rip models have a density varying with scale factor as

$$\rho = \rho_0 (a/a_0)^{-3(1+w)}. \tag{4.24}$$

For $|1 + w| \ll 1$ and a/a_0 not too far from 1, equation (4.24) behaves as

$$\rho \approx \rho_0 [1 - 3(1 + w) \ln(a/a_0)]. \tag{4.25}$$

Equation (4.12) reduces to equation (4.25) for $A/\sqrt{\rho_0} \ll 1$, with $A/\sqrt{\rho_0} = -(1 + w)$.

4.4 Disintegration

A feature of a big rip is that all bound-state systems disintegrate before the final singularity [29]. Here we show that little rip models, despite not having a final

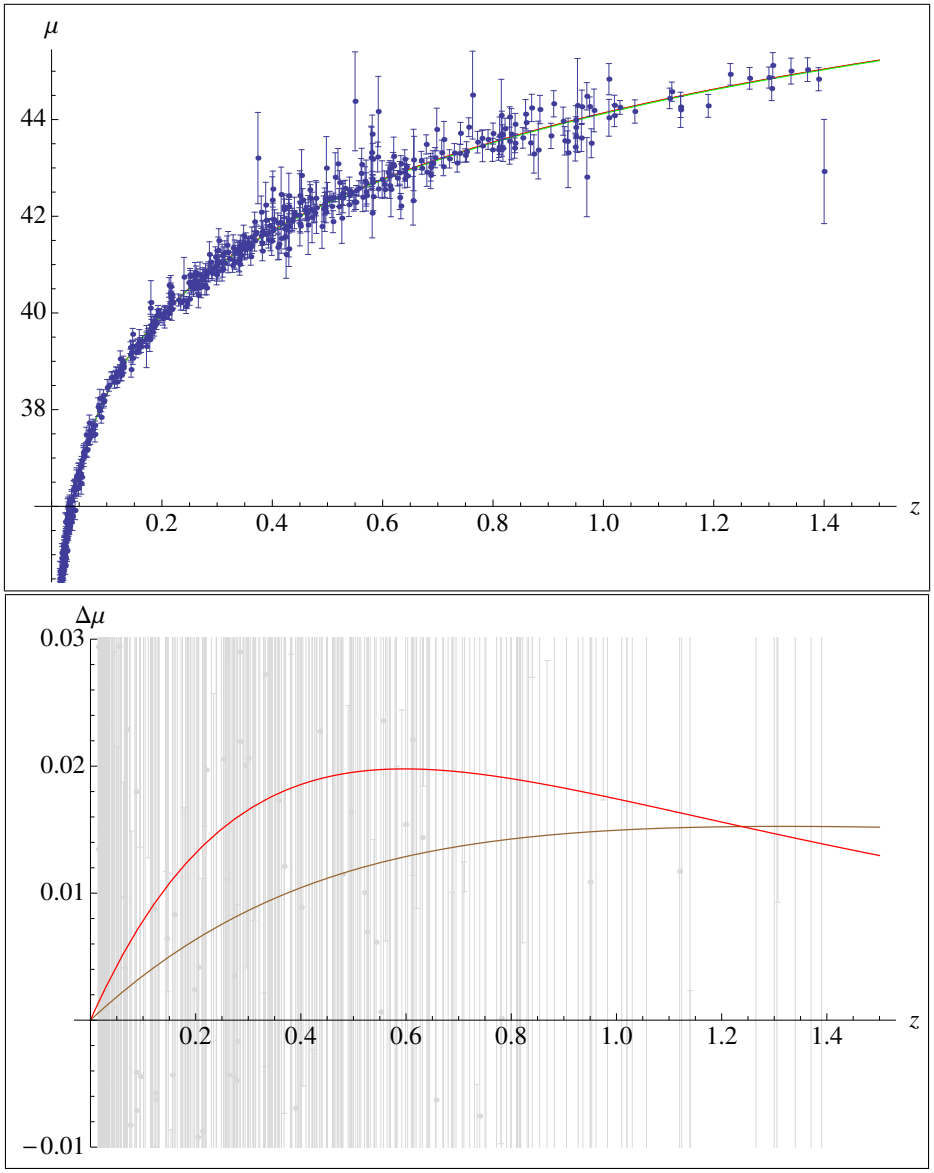

Figure 4.1: Top panel: Hubble plot of distance modulus μ versus redshift z for the ΛCDM ($w = -1$) model (green) and models 1 (brown) and 2 (red). The lines are essentially indistinguishable. Bottom panel: The ΛCDM model is subtracted from models 1 (brown) and 2 (red). The ΛCDM model is, by definition, represented by the $\Delta\mu = 0$ axis. As can be judged by the size of the error bars of the data, all are excellent fits to the supernovae data.

singularity, also produce the disintegration of bound structures. As a first approximation, the disintegration time is when the dark energy density equals the mean density of the system. A more accurate method was presented in [60]. We shall employ both methods to estimate the disintegration of the Sun-Earth system.[2] For the little rip models 1 and 2, with the best-fit parameters derived in the previous section, we find the time $t_{\odot-\oplus}$ from the present time t_0 until the Earth ($\oplus$) - Sun ($\odot$) system is disintegrated to be:

$$\text{Model 1}: \quad t_{\odot-\oplus} \simeq 8 \text{ Tyrs} \tag{4.26}$$

$$\text{Model 2}: \quad t_{\odot-\oplus} \simeq 146 \text{ Gyrs.} \tag{4.27}$$

Note that the disintegration time for model 2 is less than that of model 1, which is expected since ρ for model 2 grows faster than ρ for model 1.

It is straightforward to estimate the corresponding $t_{\odot-\oplus}$ for big rip models with constant w to be [59]

$$t_{\odot-\oplus} \simeq \left(\frac{11 \text{ Gyrs}}{|1+w|}\right), \tag{4.28}$$

and it is almost identical to t_{rip}, which is about one year later.

Clearly, little rip models can produce this disintegration either earlier or later than big rip models, depending on the exact parameters of each model. For example, by putting, $w = -1 - 10^{-3}$ in equation (4.28), we find a value of 11 Tyrs for $t_{\odot-\oplus}$, which is larger than that of models 1 and 2 in Eqs.(4.26, 4.27). In this case, disintegration occurs earlier in the little rip model than in the big rip model.

The five energy conditions (weak, null, dominant, null dominant, strong) (see, e.g., Ref. [26]) are all violated by all little rip and big rip models. A simple way

[2]When the Sun becomes a red giant in ~ 5 Gyrs, it will envelope Mercury and Venus, and (maybe) Earth [76]. Here, for the sake of making a point, we assume the Earth will continue to orbit the Sun until unbound by dark energy.

to see this is that if $w < -1$, which occurs for any rip, a boost is allowed with $(v/c)^2 > -w/c$ to an inertial frame with negative energy density. Having said that, if general relativity itself fails for length scales bigger than that of galaxies, we may not be constrained by the same energy conditions.

4.5 Discussion

In the big rip, the scale factor and density diverge in a singularity at a finite future time. In the ΛCDM model, there is no such divergence and no disintegration because the dark energy density remains constant. The little rip interpolates between these two cases; mathematically it can be represented as an infinite limit sequence which has the big rip and the ΛCDM model as its boundaries. Such models can be represented generically by a density varying with scale factor as in equation (4.19).

Physically, in the little rip, the scale factor and the density are never infinite at a finite time. Nevertheless, such models generically lead to structure disintegration at a finite time. For models consistent with current supernova observations, such disintegration can occur either earlier or later in a little rip model than in a big rip model, depending on the parameters chosen for the models. However, for a given present-day value of w, the big rip model with constant w will necessarily lead to an earlier disintegration than the little rip model with the same present-day value of w. This results from the fact that w increases monotonically in the little rip models, resulting in a smaller value for ρ at any given a than in the corresponding constant-w big rip model, and therefore, a lower expansion rate. Thus, supernova bounds on the epoch of disintegration for constant-w big rip models also apply to little rip models; one cannot simultaneously satisfy supernova constraints and hasten the onset of disintegration to an arbitrarily early time simply by iterating exponentials in the expansion law.

Furthermore, supernova data force both big rip and little rip models into a region of parameter space in which both models resemble ΛCDM. In this limit, big rip and little rip models produce essentially the same expansion law up to the present, despite having very different future evolution. Thus, current data already make it essentially impossible to determine whether or not the universe will end in a future singularity.

Finally, we remark that since the novel and speculative cyclic cosmology proposed in Ref. [77] requires only disintegration and not a singularity, such cyclicity would seem to be possible within a little rip model instead of the big rip considered in [77]. This is one potentially fruitful direction for future research.

Chapter 5

Models for Little Rip Dark Energy[1]

5.1 Introduction

The current acceleration of the universe is often attributed to dark energy, an unknown fluid with effective equation of state (EoS) parameter w close to -1. The observational data [13, 12, 75, 79] favor ΛCDM with $w = -1$. However, phantom ($w < -1$) or quintessence ($-1/3 > w > -1$) dark energy models are not excluded by observational data [80]. In both cases, it is known that the universe may evolve to a finite-time future singularity. Phantom dark energy models can lead to a singularity in which the scale factor and density become infinite at a finite time; such a singularity is called a big rip [59, 29], or Type I singularity [62]. For quintessence dark energy, one can have a singularity for which the pressure goes to infinity at a fixed time, but the scale factor and density remain finite; this is called a sudden singularity [69, 70], or a Type II singularity [62]). Alternately, the density and pressure can both become infinite with a finite scale factor at a finite time (a Type III singularity), or higher derivatives of the Hubble parameter H can diverge (a Type IV singularity) [62]. The occurrence of a singularity at a finite time in the future

[1]This chapter is taken from [78].

may lead to some inconsistencies. Several scenarios to avoid a future singularity have been proposed so far: coupling with dark matter [81], inclusion of quantum effects [82], additional changes in the equation of state [83], or special forms of modified gravity [83].

Recently, a new scenario to avoid a future singularity has been proposed in Ref. [55]. In this scenario, w is less than -1, so that the dark energy density increases with time, but w approaches -1 asymptotically and sufficiently rapidly that a singularity is avoided. This proposed non-singular cosmology was called a "little rip" because it leads to a dissolution of bound structures at some point in the future (similar to the effect of a big rip singularity). It can be realized in terms of a general fluid with a complicated EoS [62, 63, 84]. The evolution of the little rip cosmology is close to that of ΛCDM up to the present, and is similarly consistent with the observational data.

The present article is devoted to further study of the properties of the little rip cosmology. In the next section, the inertial force interpretation of the little rip is developed, and it becomes clear why a dissolution of bound structures occurs. Coupling of the little rip fluid with dark matter is considered in Section III. It is shown that as the result of such a coupling an asymptotically de Sitter universe can eventually evolve to have a little or big rip. In Section IV, the little rip cosmology is reconstructed in terms of scalar field models. Our results are summarized in Section V.

5.2 Inertial Force Interpretation of the Little Rip

As the universe expands, the relative acceleration between two points separated by a comoving distance l is given by $l\ddot{a}/a$, where a is the scale factor. An observer a comoving distance l away from a mass m will measure an inertial force on the

mass of

$$F_{\rm iner} = ml\ddot{a}/a = ml\left(\dot{H} + H^2\right) . \tag{5.1}$$

Let us assume the two particles are bound by a constant force F_0. If $F_{\rm iner}$ is positive and greater than F_0, the two particles become unbound. This is the "rip" produced by the accelerating expansion. Note that equation (5.1) shows that a rip always occurs when either H diverges or $\dot{H}$ diverges (assuming $\dot{H} > 0$). The first case corresponds to a "big rip" [28], while if H is finite, but $\dot{H}$ diverges with $\dot{H} > 0$, we have a Type II or "sudden future" singularity [69, 70, 62], which also leads to a rip. However, as noted in Ref. [55], it is possible for H, and therefore, $F_{\rm iner}$, to increase without bound and yet not produce a future singularity at a finite time; this is the little rip. Both the big rip and little rip are characterized by $F_{\rm iner} \to \infty$; the difference is that $F_{\rm iner} \to \infty$ occurs at a finite time for a big rip and as $t \to \infty$ for the little rip.

An interesting case occurs when H is finite and $\dot{H}$ diverges but is negative. In this case, even though the universe is expanding, all structures are crushed rather than ripped. An example is given by

$$H = H_0 + H_1 \left(t_c - t\right)^\alpha . \tag{5.2}$$

Here H_0 and H_1 are positive constants and α is a constant with $0 < \alpha < 1$.

By using the Friedmann equations

$$\frac{3}{\kappa^2}H^2 = \rho\,, \quad -\frac{1}{\kappa^2}\left(2\dot{H} + 3H^2\right) = p\,, \tag{5.3}$$

where $\kappa \equiv \sqrt{8\pi G}$, we may rewrite (5.1) in the following form:

$$F_{\rm iner} = -\frac{ml\kappa^2}{6}\left(\rho + 3p\right) . \tag{5.4}$$

Here $\kappa^2 = 8\pi G$ and G is Newton's gravitational constant. Not surprisingly, we see that the inertial force is sourced by the quantity $\rho + 3p$. Then if we consider the general equation of state,

$$p = -\rho + f(\rho)\,, \tag{5.5}$$

we find

$$F_{\rm iner} = \frac{ml\kappa^2}{6}\left(2\rho - 3f(\rho)\right)\,. \tag{5.6}$$

As noted in Ref. [55], when $w \to -1$ but $w < -1$, a rip can occur without a singularity. If we ignore the contribution from matter, the equation of state (EoS) parameter w of the dark energy can be expressed in terms of the Hubble rate H as

$$w = -1 - \frac{2\dot{H}}{3H^2}\,. \tag{5.7}$$

Then if $\dot{H} > 0$, we find $w < -1$.

Now consider the following example:

$$H = H_0 \mathrm{e}^{\lambda t}\,. \tag{5.8}$$

Here H_0 and λ are positive constants. Eq. (5.8) tells us that there is no curvature singularity for finite t. By using Eq. (5.7), we find

$$w = -1 - \frac{2\lambda}{3H_0}\mathrm{e}^{-\lambda t}\,, \tag{5.9}$$

and therefore $w < -1$ and $w \to -1$ when $t \to +\infty$, and w is always less than -1 when $\dot{H}$ is positive. From Eq. (5.1), we have

$$F_{\rm iner} = ml\left(\lambda H_0 \mathrm{e}^{\lambda t} + H_0^2 \mathrm{e}^{2\lambda t}\right)\,, \tag{5.10}$$

which is positive and unbounded. Thus, $F_{\rm iner}$ becomes arbitrarily large with increasing t, resulting in a little rip.

As another example, consider the model:

$$H = H_0 - H_1 \mathrm{e}^{-\lambda t} \,. \tag{5.11}$$

Here H_0, H_1, and λ are positive constants and we assume $H_0 > H_1$ and $t > 0$. Since the second term decreases when t increases, the universe goes to asymptotically de Sitter space-time. Then from Eq. (5.7), we find

$$w = -1 - \frac{2\lambda H_1 \mathrm{e}^{-\lambda t}}{3\left(H_0 - H_1 \mathrm{e}^{-\lambda t}\right)^2} \,. \tag{5.12}$$

As in the previous example, $w < -1$ and $w \to -1$ when $t \to +\infty$. For H given by Eq. (5.11), however, the inertial force, given by (5.1), is

$$F_{\rm iner} = ml \left\{ \lambda H_1 \mathrm{e}^{-\lambda t} + \left(H_0 - H_1 \mathrm{e}^{-\lambda t}\right)^2 \right\} \,, \tag{5.13}$$

which is positive but bounded and $F_{\rm iner} \to mlH_0^2$ when $t \to +\infty$. Therefore if we choose H_0, H_1, and λ small enough, we do not obtain a rip. When t becomes large, the scale factor a is given by that of the de Sitter space-time $a \sim a_0 \mathrm{e}^{H_0 t}$, and the energy density ρ has the following form:

$$\rho = \frac{3}{\kappa^2} H^2 \sim \frac{3}{\kappa^2} \left(H_0^2 - 2H_0 H_1 \mathrm{e}^{-\lambda t}\right) \sim \frac{3}{\kappa^2} \left(H_0^2 - 2H_0 H_1 \left(\frac{a}{a_0}\right)^{-\frac{\lambda}{H_0}} \right) \,, \tag{5.14}$$

which is an increasing function of a and becomes finite as $a \to \infty$.

For $t \to \infty$, Eq. (5.12) gives the asymptotic behavior of w to be

$$w \sim -1 - \frac{2\lambda H_1 \mathrm{e}^{-\lambda t}}{3H_0^2} \,, \tag{5.15}$$

which is identical with (5.9) if we replace $\lambda H_1/H_0$ with λ.

These results indicate that knowledge of the asymptotic ($t \to \infty$) behavior of $w(t)$ is insufficient to distinguish models with a rip from models which are asymptotically de Sitter. The reason for this becomes clear when we derive the expression for $\rho(t)$ as a function of $w(t)$. The evolution of ρ is given by:

$$\frac{d\rho}{dt} = -3H(\rho + p)\,, \tag{5.16}$$

which can be expressed as

$$\rho^{-3/2}\frac{d\rho}{dt} = -\sqrt{3}\kappa(1+w)\,. \tag{5.17}$$

Integrating between initial and final times t_i and t_f gives:

$$\rho_i^{-1/2} - \rho_f^{-1/2} = -\frac{\sqrt{3}}{2}\int_{t_i}^{t_f}[1+w(t)]dt\,. \tag{5.18}$$

Evolution leading to a little rip implies that $\rho_f \to \infty$ as $t_f \to \infty$, while asymptotic de Sitter evolution requires $\rho_f \to$ constant as $t_f \to \infty$. However, in either case, the integral on the right-hand side simply approaches a constant as the upper limit goes to infinity. Thus, the asymptotic functional form for $w(t)$ is not a good test of the asymptotic behavior of ρ.

On the other hand, expressing the equation of state parameter as a function of the scale factor a instead of the time t does provide a clearer test of the existence of a future rip. Equation (5.16) can be written in terms of the scale factor as

$$\frac{a}{\rho}\frac{d\rho}{da} = -3[1+w(a)]\,, \tag{5.19}$$

from which it follows that

$$\ln\left(\frac{\rho_f}{\rho_i}\right) = -3\int_{a_i}^{a_f}[1+w(a)]\frac{da}{a}\,. \tag{5.20}$$

Thus, ρ is asymptotically constant if the integral of $(1+w)/a$ converges at its upper limit, while ρ will increase without bound, leading to a rip, when the integral diverges. Then if $1+w(a)$ behaves as an inverse power of a, as in $1+w(a) \sim a^{-\epsilon}$ with arbitrary positive constant ϵ when $a \to \infty$, the integration on the right-hand side of (5.20) is finite when $a_f \to \infty$, and therefore a rip does not occur. If $1+w(a)$ vanishes more slowly than any power of a when $a \to \infty$, e.g., $1+w(a) \sim 1/\ln a$, the integration on the right-hand side of (5.20) diverges when $a_f \to \infty$, and therefore a rip is generated.

We now consider what kind of perfect fluid realizes the evolution of H in Eqs. (5.8) or (5.11). The Friedmann equations give

$$\rho = \frac{3}{\kappa^2}H^2\,, \quad \rho + p = -\frac{2}{\kappa^2}\dot{H}\,. \tag{5.21}$$

Consider first the model given by Eq. (5.8). By substituting Eq. (5.8) into Eq. (5.21) and eliminating t, we obtain:

$$(\rho+p)^2 = \frac{4\lambda^2}{3\kappa^2}\rho\,. \tag{5.22}$$

On the other hand, for the case corresponding to Eq. (5.11), we obtain:

$$\rho = \frac{3H_0^2}{\kappa^2} + \frac{3H_0}{\lambda}(\rho+p) + \frac{3\kappa^2}{4\lambda^2}(\rho+p)^2\,. \tag{5.23}$$

5.3 Coupling with Dark Matter

In Ref. [81], it was shown that the coupling of zero-pressure dark matter with phantom dark energy could avoid a big rip singularity, and the universe might evolve to asymptotic de Sitter space. Here we investigate the possibility that coupling with the dark matter could avoid a little rip. We consider the equation of state Eq. (5.22), for which a little rip occurs in the absence of such a coupling. We show that by adding a coupling with dark matter, a little rip can be avoided, and the universe can evolve to de Sitter space.

We now consider the following conservation law [81]

$$\dot{\rho} + 3H\left(\rho + p\right) = -Q\rho\,, \quad \dot{\rho}_{\rm DM} + 3H\rho_{\rm DM} = Q\rho\,. \tag{5.24}$$

Here $\rho_{\rm DM}$ is the energy density of the dark matter and Q is a positive constant. The right-hand sides in Eqs. (5.24) express the decay of the dark energy into dark matter. We assume the equation of state given in Eq. (5.22), for which a rip could occur. Then the first equation in (5.24) can be rewritten as

$$\dot{\rho} - \frac{2\lambda\sqrt{3\rho}}{\kappa}H = -Q\rho\,. \tag{5.25}$$

Note that $\rho + p < 0$ since we are considering the model $w < -1$.

We now assume the de Sitter solution where H is a constant: $H = H_0 > 0$. If we neglect the contribution from everything other than the dark energy and dark matter, the first Friedmann equation

$$\frac{3}{\kappa^2}H^2 = \rho + \rho_{\rm DM} \tag{5.26}$$

indicates that $\rho + \rho_{\rm DM}$ is a constant. Then Eq. (5.24) becomes

$$0 = 3H_0 \left(\rho + p + \rho_{\rm DM}\right) . \tag{5.27}$$

Since $H = H_0 > 0$, we find

$$\rho_{\rm DM} = -\rho - p \, . \tag{5.28}$$

Note that the above equation (5.28) can be obtained from the conservation law (5.24) and the first Friedmann equation (5.26) without using any equation of state.

Now we assume the equation of state (5.22). Combining Eqs. (5.22) and (5.28), we get

$$\rho = \frac{3\kappa^2}{4\lambda^2}\rho_{\rm DM}^2 \, . \tag{5.29}$$

Since $\rho + \rho_{\rm DM}$ is a constant, Eq. (5.29) implies that $\rho_{\rm DM}$ and therefore ρ is a constant. Then the second equation in (5.24) gives

$$\rho_{\rm DM} = \frac{4H_0\lambda^2}{\kappa^2 Q} \, , \tag{5.30}$$

and therefore, from (5.29), we find

$$\rho = \frac{12H_0^2\lambda^2}{\kappa^2 Q^2} \, . \tag{5.31}$$

Then by using the Friedmann equation (5.26), we find

$$H_0 = \frac{4\lambda^2}{3Q\left(1 - \frac{4\lambda^2}{Q^2}\right)} \, . \tag{5.32}$$

This requires

$$\frac{\lambda}{Q} < \frac{1}{2} \, . \tag{5.33}$$

By using (5.32), we can rewrite (5.30) and (5.31) as

$$\rho_{\rm DM} = \frac{16\lambda^4}{3\kappa^2 Q^2\left(1-\frac{4\lambda^2}{Q^2}\right)}\,, \quad \rho = \frac{64\lambda^6}{3\kappa^2 Q^4\left(1-\frac{4\lambda^2}{Q^2}\right)^2}\,. \tag{5.34}$$

Then we obtain

$$\frac{\rho_{\rm DM}}{\rho} = \frac{Q^2\left(1-\frac{4\lambda^2}{Q^2}\right)}{4\lambda^2}\,. \tag{5.35}$$

At the present time, $\rho_{\rm DM}/\rho \sim 1/3$, and the fact that this ratio is of order unity today is called the coincidence problem. This observed ratio can be obtained in our model when $\lambda^2/Q^2 \sim 3/16$.

De Sitter space can be realized by the a-independent energy density. The energy density of the phantom dark energy increases by the expansion but it decreases by the decay into the dark matter. On the other hand, the energy density of the dark matter decreases by the expansion but it increases by the decay of the dark energy. In the above solution, the decay of the dark energy into the dark matter balances with the expansion of the universe, and the energy densities of both the dark energy and dark matter become constant. This mechanism is essentially identical to one found in [81].

If the solution corresponding to de Sitter space-time is an attractor, the universe becomes asymptotic de Sitter space-time and any rip might be avoided. In order to investigate if the de Sitter space-time is an attractor or not, we consider the perturbation from the de Sitter solution in (5.32) and (5.34):

$$\begin{aligned} H &= \frac{4\lambda^2}{3Q\left(1-\frac{4\lambda^2}{Q^2}\right)} + \delta H\,, \quad \rho_{\rm DM} = \frac{16\lambda^4}{3\kappa^2 Q^2\left(1-\frac{4\lambda^2}{Q^2}\right)} + \delta\rho_{\rm DM}\,, \\ \rho &= \frac{64\lambda^6}{3\kappa^2 Q^4\left(1-\frac{4\lambda^2}{Q^2}\right)^2} + \delta\rho\,. \end{aligned} \tag{5.36}$$

Then the first Friedmann equation (5.26) gives

$$\frac{8\lambda^2}{\kappa^2 Q\left(1-\frac{4\lambda^2}{Q^2}\right)}\delta H = \delta\rho + \delta\rho_{\rm DM}\,. \tag{5.37}$$

The conservation laws (5.24) and (5.25) give

$$\begin{aligned}
\delta\dot{\rho} &= \frac{16\lambda^4}{\kappa^2 Q^2\left(1-\frac{4\lambda^2}{Q^2}\right)}\delta H - \frac{Q}{2}\delta\rho\,,\\
\delta\dot{\rho}_{\rm DM} &= -\frac{16\lambda^4}{\kappa^2 Q^2\left(1-\frac{4\lambda^2}{Q^2}\right)}\delta H + Q\delta\rho - \frac{4\lambda^2}{Q\left(1-\frac{4\lambda^2}{Q^2}\right)}\delta\rho_{\rm DM}\,.
\end{aligned} \tag{5.38}$$

By eliminating δH in (5.38) using (5.37), we obtain

$$\frac{d}{dt}\begin{pmatrix}\delta\rho\\ \delta\rho_{\rm DM}\end{pmatrix} = \begin{pmatrix} -\frac{Q}{2}\left(1-\frac{4\lambda^2}{Q^2}\right) & \frac{2\lambda^2}{Q}\\ Q\left(1-\frac{2\lambda^2}{Q^2}\right) & -\frac{\frac{2\lambda^2}{Q}\left(3-\frac{4\lambda^2}{Q^2}\right)}{1-\frac{4\lambda^2}{Q^2}}\end{pmatrix}\begin{pmatrix}\delta\rho\\ \delta\rho_{\rm DM}\end{pmatrix}\,. \tag{5.39}$$

In order for the de Sitter solution in (5.32) and (5.34) to be stable, all the eigenvalues of the matrix in (5.39) should be negative, which requires the trace of the matrix to be negative and the determinant to be positive, giving

$$-\frac{Q}{2}\left(1-\frac{4\lambda^2}{Q^2}\right) - \frac{\frac{2\lambda^2}{Q}\left(3-\frac{4\lambda^2}{Q^2}\right)}{1-\frac{4\lambda^2}{Q^2}} < 0\,, \quad \lambda^2 > 0\,. \tag{5.40}$$

The second condition can be trivially satisfied, and the first condition is also satisfied as long as (5.33) is satisfied. Therefore the de Sitter solution in (5.32) and (5.34) is stable and therefore an attractor. This tells us that the coupling of the dark matter with the dark energy as in (5.24) eliminates the little rip.

Thus, if the universe where the dark energy dominates is realized, the universe will expand as in (5.8). If there is an interaction as given in (5.24), the dark energy

decay into dark matter will yield asymptotic de Sitter space-time corresponding to Eq. (5.32).

5.4 Scalar Field Little Rip Cosmology

5.4.1 Minimally Coupled Phantom Models

First consider a minimally coupled phantom field ϕ which obeys the equation of motion

$$\ddot{\phi} + 3H\dot{\phi} - V'(\phi) = 0\,, \tag{5.41}$$

where the prime denotes the derivative with respect to ϕ. A field evolving according to equation (5.41) rolls uphill in the potential. In what follows, we assume a monotonically increasing potential $V(\phi)$. If this is not the case, then it is possible for the field to become trapped in a local maximum of the potential, resulting in asymptotic de Sitter evolution.

Kujat, Scherrer, and Sen [68] derived the conditions on $V(\phi)$ to avoid a big rip, namely $V'/V \to 0$ as $\phi \to \infty$, and

$$\int \frac{\sqrt{V(\phi)}}{V'(\phi)} d\phi \to \infty\,. \tag{5.42}$$

When these conditions are satisfied, w approaches -1 sufficiently rapidly that a big rip is avoided.

We now extend this argument to determine the conditions necessary to avoid a little rip. Clearly, we will have $\rho \to$ constant if $V(\phi)$ is bounded from above, so that $V(\phi) \to V_0$ (where V_0 is a constant) as $\phi \to \infty$. We can show that this is also a necessary condition. Suppose that $V(\phi)$ is not bounded from above, so that $V(\phi) \to \infty$ as $\phi \to \infty$. Then the only way for the density of the scalar field to

remain bounded is if the field "freezes" at some fixed value ϕ_0. However, this is clearly impossible from equation (5.41), since it would require $\ddot{\phi} = \dot{\phi} = 0$ while $V'(\phi) \neq 0$. Thus, boundedness of the potential determines the boundary between little rip and asymptotic de Sitter evolution. Phantom scalar field models with bounded potentials have been discussed previously in Ref. [82].

5.4.2 Scalar-Tensor Models

Using the formulation in Ref. [85], we now consider what kind of scalar-tensor model, with an action given by

$$S = \int d^4x\sqrt{-g}\left\{\frac{1}{2\kappa^2}R - \frac{1}{2}\omega(\phi)\partial_\mu\phi\partial^\mu\phi - V(\phi)\right\}, \tag{5.43}$$

can realize the evolution of H given in Eqs. (5.8) or (5.11). Here $\omega(\phi)$ and $V(\phi)$ are functions of the scalar field ϕ. Since the corresponding fluid is phantom with $w < -1$, the scalar field must be a ghost with a non-canonical kinetic term. If we consider the model where $\omega(\phi)$ and $V(\phi)$ are given by a single function $f(\phi)$ as follows,

$$\omega(\phi) = -\frac{2}{\kappa^2}f''(\phi)\,, \quad V(\phi) = \frac{1}{\kappa^2}\left(3f'(\phi)^2 + f''(\phi)\right), \tag{5.44}$$

the exact solution of the Friedmann equations has the following form:

$$\phi = t\,, \quad H = f'(t)\,. \tag{5.45}$$

Then for the model given by Eq. (5.8), we find

$$\omega(\phi) = -\frac{2\lambda H_0}{\kappa^2}\mathrm{e}^{\lambda\phi}\,, \quad V(\phi) = \frac{1}{\kappa^2}\left(3H_0^2\mathrm{e}^{2\lambda\phi} + \lambda H_0\mathrm{e}^{\lambda\phi}\right). \tag{5.46}$$

Furthermore, if we redefine the scalar field ϕ to φ by

$$\varphi = \frac{2\mathrm{e}^{\frac{\lambda}{2}\phi}}{\kappa}\sqrt{\frac{2H_0}{\lambda}}\,, \tag{5.47}$$

we find that the action (5.43) has the following form:

$$S = \int d^4x\sqrt{-g}\left\{\frac{1}{2\kappa^2}R + \frac{1}{2}\partial_\mu\varphi\partial^\mu\varphi - \frac{3\lambda^2\kappa^2}{64}\varphi^4 - \frac{\lambda^2}{8}\varphi^2\right\}. \tag{5.48}$$

Note that in the action (5.48), H_0 does not appear. This is because the shift of t in (5.8) effectively changes H_0. The parameter A in [55] corresponds to $2\lambda/\sqrt{3}$ in (5.8) and is bounded as $2.74\times10^{-3}\,\mathrm{Gyr}^{-1} \leq A \leq 9.67\times10^{-3}\,\mathrm{Gyr}^{-1}$, or $2.37\times10^{-3}\,\mathrm{Gyr}^{-1} \leq \lambda \leq 8.37\times10^{-3}\,\mathrm{Gyr}^{-1}$, by the results of the Supernova Cosmology Project [74]. In [55], it was shown that the model defined by Eq. (5.8) can give behavior of the distance modulus versus redshift almost identical to that of ΛCDM, so this model can be made consistent with observational data.

As in Ref. [55], we can generalize the behavior of this model to

$$H = H_0\mathrm{e}^{C\mathrm{e}^{\lambda t}}\,. \tag{5.49}$$

Here H_0, C, and λ are positive constants. Then we find

$$\omega(\phi) = -\frac{2}{\kappa^2}H_0C\lambda\mathrm{e}^{C\mathrm{e}^{\lambda\phi}}\mathrm{e}^{\lambda\phi}\,,\quad V(\phi) = \frac{1}{\kappa^2}\left(3H_0^2\mathrm{e}^{2C\mathrm{e}^{\lambda\phi}} + H_0C\lambda\mathrm{e}^{C\mathrm{e}^{\lambda\phi}}\mathrm{e}^{\lambda\phi}\right). \tag{5.50}$$

If we redefine the scalar field ϕ to φ by

$$\begin{aligned}\varphi &= \frac{\sqrt{2H_0C\lambda}}{\kappa}\int d\phi\mathrm{e}^{\frac{C}{2}\mathrm{e}^{\lambda\phi}}\mathrm{e}^{\frac{\lambda}{2}\phi} = \frac{1}{\kappa}\sqrt{\frac{8H_0C}{\lambda}}\int^{\mathrm{e}^{\frac{\lambda}{2}\phi}} dx\mathrm{e}^{\frac{C}{2}x^2}\\ &= \frac{2}{\kappa}\sqrt{\frac{H_0\pi}{\lambda}}\mathrm{Erfi}\left[\sqrt{\frac{C}{2}}\mathrm{e}^{\frac{\lambda}{2}\phi}\right],\end{aligned} \tag{5.51}$$

we may obtain the action where the kinetic term of the scalar field φ is $+\frac{1}{2}\partial_\mu\varphi\partial^\mu\varphi$. In (5.51), $\mathrm{Erfi}[x] = \mathrm{Erf}[ix]/i$ with $i^2 = -1$, where $\mathrm{Erf}[x]$ is the error function. In [55], it was shown that the model given by Eq. (5.49) can also be consistent with the observations.

As in Ref. [55], we can easily find models which show more complicated behavior of H such as

$$H = H_0 \mathrm{e}^{C_0 \mathrm{e}^{C_1 \mathrm{e}^{C_2 \mathrm{e}^{\lambda t}}}} \,. \tag{5.52}$$

On the other hand, in the model given by Eq. (5.11), we find

$$\omega(\phi) = -\frac{2\lambda H_1}{\kappa^2}\mathrm{e}^{-\lambda\phi}\,, \quad V(\phi) = \frac{1}{\kappa^2}\left\{3\left(H_0 - H_1\mathrm{e}^{-\lambda\phi}\right)^2 + \lambda H_1 \mathrm{e}^{-\lambda\phi}\right\}\,, \tag{5.53}$$

and by the redefinition

$$\varphi = \frac{2\mathrm{e}^{-\frac{\lambda}{2}\phi}}{\kappa}\sqrt{\frac{2H_1}{\lambda}}\,, \tag{5.54}$$

we find that the action (5.43) has the following form:

$$S = \int d^4x\sqrt{-g}\left\{\frac{1}{2\kappa^2}R + \frac{1}{2}\partial_\mu\varphi\partial^\mu\varphi - \frac{1}{\kappa^2}\left[3\left(H_0 - \frac{\lambda\kappa^2}{8}\varphi^2\right)^2 + \frac{\lambda^2\kappa^2}{8}\varphi^2\right]\right\}\,. \tag{5.55}$$

In the action given by Eq. (5.55), H_1 does not appear. This is because the shift of t in (5.11) effectively changes H_1.

Eq. (5.47) shows that in the infinite future $t = \phi \to +\infty$, φ also goes to infinity, that is, the scalar field climbs up the potential to infinity. This climbing up the potential makes the Hubble rate grow and generates a rip due to the inertial force (5.1). On the other hand, Eq. (5.54) tells us that when $\phi \to +\infty$, φ vanishes. Note that the potential in (5.55) is a double well potential similar to the potential of the Higgs field, and $\varphi = 0$ corresponds to the local maximum of the potential. Therefore, in the model given by (5.55), the scalar field climbs up the potential

and arrives at the local maximum after an infinite time. The behavior of the scalar field is different from that of the canonical scalar field, which usually rolls down the potential. This phenomenon of how the scalar field climbs up the potential occurs due to the non-canonical kinetic term. For the canonical scalar field φ_c, the field equation has the form of $\nabla_t^2\varphi_c = -V'(\phi)$, but if the sign of the kinetic term is changed, we obtain $\nabla_t^2\varphi_c = V'(\phi)$ for a non-canonical scalar field. That is, the sign of the "force" is effectively changed.

We now investigate the stability of the solution (5.45) in the model given by Eqs. (5.43) and (5.44) by considering the perturbation from the solution (5.45):

$$\phi = t + \delta\phi(t)\,, \quad H = f'(t) + \delta h(t)\,. \tag{5.56}$$

By using the Friedmann equations

$$\frac{3}{\kappa^2}H^2 = \frac{1}{2}\omega(\phi)\dot{\phi}^2 + V(\phi)\,, \quad -\frac{1}{\kappa^2}\left(2\dot{H} + 3H^2\right) = \frac{1}{2}\omega(\phi)\dot{\phi}^2 - V(\phi)\,, \tag{5.57}$$

we find

$$\frac{d}{dt}\begin{pmatrix}\delta h\\ \delta\phi\end{pmatrix} = \begin{pmatrix}-6f'(t) & 6f'(t)f''(t) + f'''(t)\\ -3\frac{f'(t)}{f''(t)} & 3f'(t)\end{pmatrix}\begin{pmatrix}\delta h\\ \delta\phi\end{pmatrix}\,. \tag{5.58}$$

In order for the solution (5.45) to be stable, all the eigenvalues of the matrix in (5.58) should be negative, which requires the trace of the matrix to be negative and the determinant to be positive, giving

$$-3f'(t) < 0\,, \quad 3\frac{f'(t)f'''(t)}{f''(t)} > 0\,. \tag{5.59}$$

The first condition is trivially satisfied in the expanding universe since $f'(t) =$

$H > 0$. If the universe is in the phantom phase, where $f''(t) = \dot{H} > 0$, the second condition reduces to $f'''(t) = \ddot{H} > 0$. Then the model corresponding to (5.11) is unstable but the model corresponding to (5.8) is stable. There are no local maxima in the potential in (5.48), so one would expect the field to climb the potential well to infinity, generating a rip. In general, in a model which generates a big or little rip, H goes to infinity, which requires $\ddot{H} > 0$. Therefore in the scalar field model generating a big or little rip, the solution corresponding to the rip is stable, and models that are asymptotically de Sitter can eventually evolve to have a rip.

5.5 Including Matter

In the previous sections, we have neglected the contribution from matter except for dark matter in Sec. 5.3. In this section, we now consider the effect of additional matter components. We assume each component has a constant EoS parameter $w_{\rm m}^i$. Then the energy density and pressure contributed by all of these components can be expressed as

$$\rho_{\rm m} = \sum_i \rho_0^i a^{-3\left(1+w_{\rm m}^i\right)}\,, \quad p_{\rm m} = \sum_i w_i \rho_0^i a^{-3\left(1+w_{\rm m}^i\right)}\,. \tag{5.60}$$

Here the ρ_0^i's are constants. Even including these additional matter components, we can construct the scalar-tensor model realizing the evolution of H by, instead of (5.44),

$$\begin{aligned}
\omega(\phi) &= -\frac{2}{\kappa^2} g''(\phi) - \sum_i \frac{w_{\rm m}^i + 1}{2} \rho_0^i a_0^{-3(1+w_{\rm m}^i)} {\rm e}^{-3(1+w_{\rm m}^i)g(\phi)}\,, \\
V(\phi) &= \frac{1}{\kappa^2}\left(3g'(\phi)^2 + g''(\phi)\right) + \sum_i \frac{w_{\rm m}^i - 1}{2} \rho_0^i a_0^{-3(1+w_{\rm m}^i)} {\rm e}^{-3(1+w_{\rm m}^i)g(\phi)}\,.
\end{aligned} \tag{5.61}$$

Then the solution of the Friedmann equations (5.3) is given by

$$\phi = t\,, \quad H = g'(t)\,, \quad \left(a = a_0 \mathrm{e}^{g(t)}\right)\,. \tag{5.62}$$

We may consider the example of (5.8), which gives

$$a(t) = a_0 \mathrm{e}^{\frac{H_0}{\lambda}\mathrm{e}^{\lambda t}}\,. \tag{5.63}$$

Then by using the Friedmann equations (5.3), we find the EoS parameter $w_{\rm DE}$ corresponding to the dark energy is given by

$$\begin{aligned} w_{\rm DE} &= \frac{\frac{3}{\kappa^2}H^2 - \rho_{\rm m}}{-\frac{1}{\kappa^2}\left(2\dot{H} + 3H^2\right) - p_{\rm m}} \\ &= \frac{\frac{3}{\kappa^2}H_0^2\mathrm{e}^{2\lambda t} - \sum_i \rho_0^i a_0^{-3\left(1+w_{\rm m}^i\right)}\mathrm{e}^{-\frac{3\left(1+w_{\rm m}^i\right)H_0}{\lambda}\mathrm{e}^{\lambda t}}}{-\frac{1}{\kappa^2}\left(2\lambda H_0\mathrm{e}^{\lambda t} + 3H_0^2\mathrm{e}^{2\lambda t}\right) - \sum_i w_{\rm m}^i \rho_0^i a_0^{-3(1+w_{\rm m}^i)}\mathrm{e}^{-\frac{3\left(1+w_{\rm m}^i\right)H_0}{\lambda}\mathrm{e}^{\lambda t}}}\,. \end{aligned} \tag{5.64}$$

When t becomes large, the contribution from the matter components decreases rapidly and $w_{\rm DE}$ in (5.64) coincides with w in (5.9). The density parameter $\Omega_{\rm DE}$ of the dark energy is also given by

$$\Omega_{\rm DE} = \frac{\frac{3}{\kappa^2}H^2 - \rho_{\rm m}}{\frac{3}{\kappa^2}H^2} = 1 - \frac{\kappa^2}{3H_0^2}\sum_i \rho_0^i a_0^{-3\left(1+w_{\rm m}^i\right)}\mathrm{e}^{-\frac{3\left(1+w_{\rm m}^i\right)H_0}{\lambda}\mathrm{e}^{\lambda t} - 2\lambda t}\,, \tag{5.65}$$

which rapidly goes to unity when t becomes large. It would be interesting to consider the cosmological perturbation in the model including the contribution from these matter components.

Let $t = 0$ represent the present. We now assume the matter consists only of dust with a vanishing EoS parameter. Then we find $\rho_{\rm m} = \rho_0 a_0^{-3}\mathrm{e}^{-\frac{3H_0}{\lambda}}$ and $p_{\rm m} = 0$. Since $\Omega_{\rm DE} = 0.74$, we find $\rho_{\rm m} = 0.26 \times \frac{3H_0^2}{\kappa^2}$ by using (5.65). Since H_0 is the Hubble

parameter in the present universe, we find $H_0 = 7.24 \times 10^{-2}\,\mathrm{Gyr}^{-1}$ ($\approx 70\,\mathrm{km/s\,Mpc}$). Since $2.37 \times 10^{-3}\,\mathrm{Gyr}^{-1} \leq \lambda \leq 8.37 \times 10^{-3}\,\mathrm{Gyr}^{-1}$ (see below (5.48)), by using (5.64), we find $-0.97 < w_{\mathrm{DE}} < -0.72$, which could be consistent with the observed value $w_{\mathrm{DE}} = -0.972^{+0.061}_{-0.060}$.

5.6 Discussion

Little rip models provide an evolution for the universe intermediate between asymptotic de Sitter expansion and models with a big rip singularity. We have shown that the EoS parameter w as a function of time is a less useful diagnostic of such behavior than is w as a function of the scale factor. As for the case of big rip singularities, a little rip can be avoided if the dark energy is coupled to the dark matter so that energy flows from the dark energy to the dark matter. Minimally coupled phantom scalar field models can lead to viable little rip cosmologies. The models we investigated that yield little rip evolution turned out to be stable against small perturbations, and we found that big rip evolution is also consistent with the conditions for stability. For phantom field models, rip-like behavior is an attractor.

It is interesting that it was recently demonstrated that the little rip cosmology may be realized by a viscous fluid [86]. It turns out that the viscous little rip cosmology can also be stable.

Scalar little rip dark energy represents a natural alternative to the ΛCDM model, which also leads to a non-singular cosmology. It remains to consider the coupling of such a model with matter and to confront its predictions with observations.

It is known [26, 27] that in a local frame with a flat background, a classical field theory with $w < -1$ has a negative kinetic energy term, and the corresponding quantum field theory has a tachyonic instability and a vacuum decay lifetime which appears finite, although possibly greater than the age of the universe. Our

result shows that in the presence of a rip, the space-time expansion is so fast that this tachyonic instability does not have time to destabilize the global geometry and shows, interestingly, that the extraordinary conditions of a little rip can lead to an infinite lifetime.

Chapter 6

The Pseudo-Rip[1]

6.1 Introduction

Time is an elusive concept of great interest to all physicists since it underlies all dynamical systems. Although we can measure time on everyday scales with exquisite precision, the deeper meaning of time may be addressed only by study of the origin and fate of the universe.

Current observations [13, 12, 88, 89] strongly suggest that the universe is dominated by a negative-pressure component, dubbed dark energy. This component can be characterized by an equation of state parameter w, which is simply the ratio of the pressure to the density: $w = p/\rho$; for example, a cosmological constant corresponds to $w = -1$. While it is often assumed that $w \geq -1$ in accordance with the weak energy condition, it has long been known [28] that the observations are consistent with $w < -1$, which corresponds to a dark energy density that increases with time t and scale factor a. If the density increases monotonically in the future, then the universe can undergo a future singularity, called the "big rip," for which $\rho \to \infty$ and $a \to \infty$ at a finite time. Shortly before this singularity is reached,

[1]This chapter is taken from [87].

bound structures are disintegrated by the expansion [29].

Note, however, that a dark energy component with a monotonically increasing density that is unbounded from above does not lead inevitably to a future singularity, although it does ultimately lead to the dissolution of all bound structures. Such models, dubbed "little rip" models, were first examined in detail by Frampton et al. [55], who derived the boundary between big rip and little rip models in terms of $\rho(a)$. Properties of little rip models were further investigated in Ref. [78].

Here we investigate a different set of models, in which the density of the dark energy increases monotonically with scale factor but is bounded from above by some limiting density, ρ_∞. Such models can still lead to a dissolution of bound structures for a sufficiently strong inertial force (which we will define), so we dub these models "pseudo-rip" models. This allows us, in the context of monotonically increasing ρ, to distinguish three distinct cosmic futures: the big rip, little rip, and pseudo-rip. (Note that models for which $\rho(a)$ is not monotonic are physically less plausible, and it is more difficult to make any sort of general statement about such models). While the dissolution of bound structures is inevitable in the big rip and little rip scenarios, it may or may not occur in a pseudo-rip, depending on the model parameters.

In the next section, we provide the definition of the pseudo-rip and examine the conditions necessary to dissolve bound structures. We then examine two specific functional forms of the dark energy density and discuss scalar field realizations of pseudo-rip models. We assume a flat FLRW metric and $c = 1$ throughout.

6.2 Definition of Pseudo-Rip

Before defining the pseudo-rip, we suggest a compact way to classify all rips. We find it useful to classify ripping behavior by means of the Hubble parameter $H(t)$.

By ripping behavior, we mean any future evolution which can lead to disintegration of structure in the form of bound systems by virtue of the strong inertial force due to dark energy.

Given the Hubble parameter $H(t)$ for $t \geq t_0$, where t_0 is the present time, the density $\rho(t)$ and pressure $p(t)$ are:

$$\rho(t) = \left(\frac{3}{8\pi G}\right) H(t)^2, \tag{6.1}$$

$$p(t) = -\left(\frac{1}{8\pi G}\right)\left[2\dot{H}(t) + 3H(t)^2\right]. \tag{6.2}$$

The big rip is defined by

$$H(t) \longrightarrow +\infty, \quad t \longrightarrow t_{rip} < \infty. \tag{6.3}$$

In a big rip, all bound structures dissociate in a finite time in the future, and space-time "rips apart" at a finite time in the future, i.e., the scale factor of the FLRW metric goes to infinity at $t = t_{rip}$ [29]. The little rip is defined by

$$H(t) \longrightarrow +\infty, \quad t \to +\infty. \tag{6.4}$$

The little rip dissociates all bound structures, but the strength of the dark energy is not enough to rip apart space-time as there is no finite-time singularity.

An excellent fit to all cosmological data is provided by the ΛCDM model which, in present parlance, is a "no-rip" model defined by

$$H(t) = H(t_0). \tag{6.5}$$

There remains just one additional possibility for monotonically increasing $H(t)$, namely

$$H(t) \longrightarrow H_\infty < \infty, \quad t \to +\infty, \tag{6.6}$$

where H_∞ is a constant. Equation (6.6) defines the pseudo-rip, the subject of the present article. A pseudo-rip dissociates bound structures that are held together by a binding force at or below a particular threshold that depends on the inertial force in the model. Eqs.(6.3)-(6.6) clearly exhaust all possibilities for a monotonically increasing $H(t)$, i.e., a monotonically increasing dark energy density $\rho(a)$.

The equations for monotonically increasing $H(t)$ are the same for $\rho(t)$ *mutatis mutandis*. Pressure $p(t) \longrightarrow -\rho(t)$ as $t \longrightarrow \infty$, provided $\dot{H}(t) \longrightarrow 0$ on the right-hand side of Eq.(6.2), which is the case for a pseudo-rip model.

Our division of the future evolution into the categories of big rip, little rip, and pseudo-rip represents a different set of models than those examined in Ref. [62, 63], which provided a classification scheme for future singularities. Our scheme represents a classification of all models with monotonically increasing dark energy density, for which the scale factor a goes smoothly to infinity, at either finite or infinite time, and for which there are no singularities in the derivatives of H unless H itself is singular. In our scheme, the big rip encompasses the type I singularity of Ref. [62, 63], while the type II, III, and IV singularities lie outside the types of models considered in our classification scheme. The little rip and pseudo-rip models are by definition non-singular, so they fall outside of the purview of Ref. [62, 63].

The inertial force F_{inert} on a mass m as seen by a gravitational source separated

by a comoving distance l is given by [78]

$$\begin{aligned} F_{inert} &= ml(\dot{H}(t) + H(t)^2) \\ &= -ml\frac{4\pi G}{3}(\rho(a) + 3p(a)) \\ &= ml\frac{4\pi G}{3}(2\rho(a) + \rho'(a)a). \end{aligned} \tag{6.7}$$

For simplicity, we set the scale factor at the present time $a_0 = a(t_0) = 1$. A bound structure dissociates when the inertial force, dominated by dark energy, grows in the future to equal the force holding together the bound structure in question. For a pseudo-rip, F_{inert} is asymptotically finite.

However, if the bound structure is massive enough to significantly affect the local space-time metric, it is not accurate to express F_{inert} in terms of the FLRW metric. A more accurate method and local metric is employed in [60], and we use their method to calculate the disintegration times for the Milky Way and the Earth-Sun system.

We analyze two psuedo-rip parameterizations for dark energy density, models 1 and 2, each as a function of the scale factor $a(t)$ with other parameters.

6.3 Model 1

Model 1 is defined by

$$\rho_1(a, B, f, s) = \rho_0 \frac{\ln[\frac{1}{f+\frac{1}{a}} + \frac{1}{B}]^s}{\ln[\frac{1}{f+1} + \frac{1}{B}]^s}, \tag{6.8}$$

where ρ_0 is the present value of the dark energy density. Note that ρ_1 is normalized to be ρ_0 at $a = 1$, which we define to represent the present. Then $\rho_1(a, B, f, s)$ is a function of the scale parameter $a(t)$ and of three other parameters B, f, and s. It is

most convenient to fix f and s, which mostly control the strength of the rip, and to keep B as a free paramater for fitting the supernova data.

We fix f and s to specify how powerful the psuedo-rip should be. The remaining free parameter is chosen to make a best fit to the latest supernova data from the Supernova Cosmology Project [74] with a reduced χ^2 of $\simeq 0.98$.

As examples of bound states we consider the Milky Way (MW), the Earth-Sun system (ES), the hydrogen atom (H atom), and the proton. The first two, MW and ES, are gravitationally bound, while for the H atom and proton, we must carefully consider the electromagnetic and strong color forces respectively. In all cases the dark energy density increases monotonically from ρ_0 at the present time to an asymptotic value. Depending on the parameters B, f, and s, the inertial force can successively disintegrate the MW, the ES, the H atom and the proton.

In different cases, some of these bounds systems will be disintegrated and not others. If none of them are disintegrated, we shall refer to such a pseudo-rip as a "failed rip."

In Fig. (6.1) we show five examples of the scaled F_{inert} for $\rho_1(a)$, which include the matter and radiation contributions. Because of these contributions, the curves go to negative infinity as a goes to 0, and the x-intercepts are values of $a < 1$ at which dark energy domination begins. Going from bottom to top, the curves represent respectively a failed rip; a pseudo-rip which disintegrates only the MW; a pseudo-rip which breaks apart the MW and ES; a pseudo-rip which destroys the MW, ES, and H atom; and the highest curve is for a pseudo-rip which succeeds in ripping apart all four of the MW, ES, H atom, and proton. Note that, unlike a little rip, the asymptotic value of $\rho_1(a)$ as $a \longrightarrow \infty$ is finite.

For a given pseudo-rip model with monotonically increasing dark energy density $\rho_{DE}(a)$, the structures with bigger binding forces disintegrate after those with

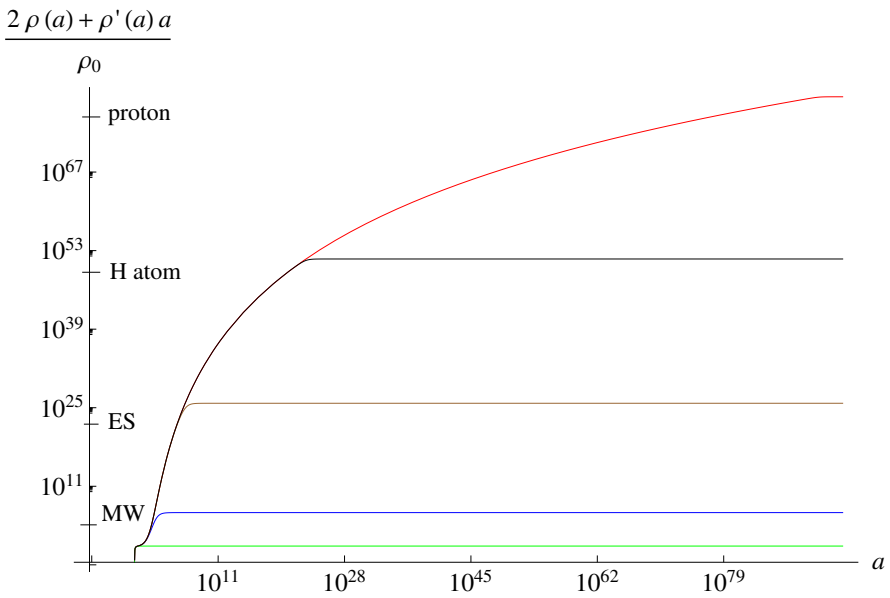

Figure 6.1: Plotted from the innermost to the outermost curve is the scaled F_{inert} for $\rho_1(a, 0.29, 10, 48)$, $\rho_1(a, 0.0108, 0.003, 48)$, $\rho_1(a, 0.01078, 2 \times 10^{-7}, 48)$, $\rho_1(a, 0.01078, 10^{-23}, 48)$, and $\rho_1(a, 0.0108, 10^{-92}, 48)$ respectively, for Model 1, given by Eq. (6.8). Each curve was fitted to supernova data with the extra constraint that $B \geq 0$. The values necessary for structural disintegration are indicated. From the innermost curve to the outermost: failed rip; $t_{MW} - t_0 = 9.2 \times 10^4$ Gyr; $t_{ES} - t_0 = 1.6 \times 10^9$ Gyr; $t_{Hatom} - t_0 = 1.3 \times 10^{33}$ Gyr; $t_{proton} - t_0 = 3.8 \times 10^{117}$ Gyr.

smaller binding forces. But a particular ρ_1 can be constructed such that it leads to, for example, the disintegration of the proton before another ρ_1 disintegrates the Milky Way.

Notice that the more violent the pseudo-rip is required to be, the more extremely small the f parameter is. One may counteract this fine tuning of f by, for example, introducing new factors into the model that help ρ_1 grow faster while still leaving it asymptotically finite. One such factor could be $(\frac{a+q}{a+2q}\frac{1+2q}{1+q})^w$. Such a factor is 1 when $a = 1$, so ρ_1 is still ρ_0 at the present time. The new parameters q and w can avoid the fine tuning.

6.4 Model 2

Model 2 is defined by

$$\rho_2(a, A, n, m) = \rho_0 \frac{A}{2}(\tan^{-1}(a-n) - \tan^{-1}(1-n) + 1)^m. \tag{6.9}$$

Like ρ_1, ρ_2 is normalized to be ρ_0 at $a = 1$. Then $\rho_2(a, A, n, m)$ is a function of the scale factor $a(t)$ and of three other parameters A, n, and m. It is most convenient to fix n and m, which mostly control the strength of the rip, and to keep A as a free paramater for fitting the supernova data. So we fix n and m to specify how powerful the psuedo-rip should be, and the remaining free parameter is chosen to make a best fit to the latest supernova data from the Supernova Cosmology Project [74] with a reduced χ^2 of $\simeq 0.98$.

In Fig. (6.2), we plot five examples of the scaled F_{inert} for $\rho_2(a)$, which include the contributions from matter and radiation. Just as in Fig. (6.1), the contributions cause the curves to approach negative infinity as a goes to 0, and the x-intercepts are values of $a < 1$ at which dark energy domination begins. The bottom curve exhibits a failed rip, while the others show pseudo-rips of various strengths. As was mentioned for Model 1, we see from Fig. (6.2) that the disintegration time for the proton for a particular ρ_2 can be sooner than the disintegration time for the Milky Way for another ρ_2.

Note in Fig. (6.2) that each F_{inert} has a local maximum. Because of this bump, $\rho_2(a \to \infty)$ is less than the maximum value of ρ_2. So it is possible, for particular parameterizations, for F_{inert} to reach the level of the binding force of a bound structure and then decrease, allowing the structure to possibly come back together. In principle, a pseudo-rip model can have F_{inert} with an arbitrary number of local maxima that give structures the chance to dissociate and reform multiple times.

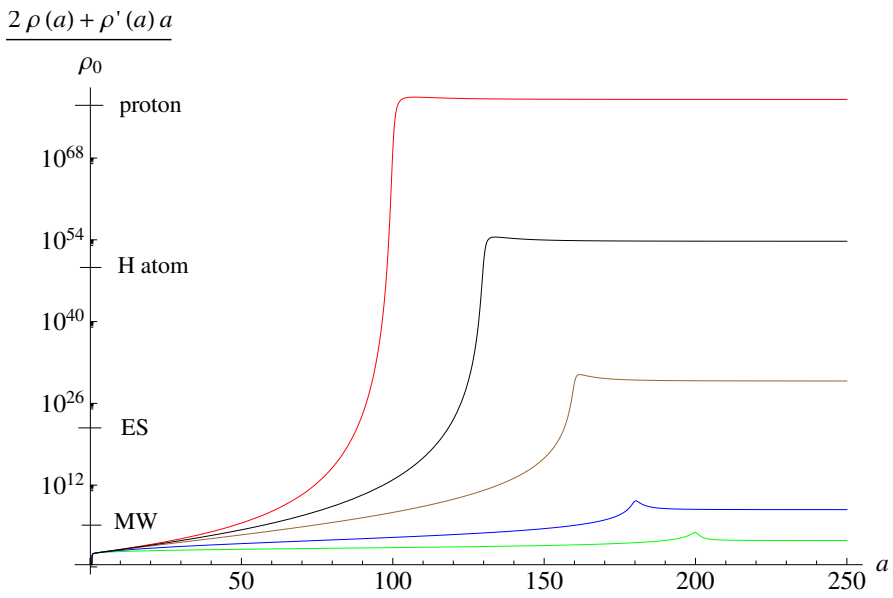

Figure 6.2: Plotted from the innermost to the outermost curve is the scaled F_{inert} for $\rho_2(a, 17481.3, 200, 0.5)$, $\rho_2(a, 3601.31, 180, 2)$, $\rho_2(a, 571.1, 160, 10)$, $\rho_2(a, 171.045, 130, 22)$, and $\rho_2(a, 55.45, 100, 40)$ respectively, for Model 2, given by Eq. (6.9). Each curve was fitted to supernova data. The values necessary for structural disintegration are indicated. As explained in the text, disintegration times from different models should not be directly compared. From the innermost curve to the outermost: failed rip; $t_{MW} - t_0 = 45$ Gyr; $t_{ES} - t_0 = 40$ Gyr; $t_{Hatom} - t_0 = 39$ Gyr; $t_{proton} - t_0 = 38$ Gyr.

All this can be achieved using a functional form for dark energy density that is monotonically increasing. However, all the examples shown in Fig. (6.2) have their asymptotic values higher than the values necessary to rip apart the structures mentioned in the plot.

6.5 Scalar Field Realizations

One possible realization of pseudo-rip models is a minimally-coupled phantom model, i.e., one that involves a scalar field with a negative kinetic term. The equation of motion for such a field is

$$\ddot{\phi} + 3H\dot{\phi} - V'(\phi) = 0\,, \tag{6.10}$$

where the dot is a time derivative, and the prime denotes the derivative with respect to ϕ. A field obeying this equation of motion rolls "uphill" in the potential.

It is clear that a sufficient condition for a pseudo-rip is that $V(\phi) \to V_0$ (where V_0 is a constant) as $\phi \to \infty$, and in Ref. [78] it was shown that this is also a necessary condition for a monotonic potential. In this case, we simply have $\rho_\infty = V_0$. If the potential is not monotonic, the density of the scalar field can also approach a constant asymptotically if the field gets trapped in a local maximum with $V = V_0$. Phantom fields with bounded potentials have been discussed previously in Ref. [82].

Note, however, that our discussion of pseudo-rips is much more general than the specific example provided by phantom field models. Phantom fields represent only a single possible realization of this much more general class of models for the asymptotic expansion of the universe.

6.6 Discussion

We have described merely two illustrative models of the pseudo-rip. Obviously, there is an infinite number of possibilities.

A failed rip will disintegrate nothing because the inertial force will not reach a high enough magnitude. Model 1 exemplifies a pseudo-rip model which can variously disintegrate between one and all four of the chosen systems while ρ_1 asymptotes to a finite density, which implies a finite inertial force, as the scale factor $a(t)$ approaches infinity. As can be seen from Fig. (6.1), these quantities plateau to a constant value after the last disintegration has taken place.

We included Model 2 as a particularly interesting example in which the inertial force rises relatively abruptly before it plateaus, as shown in Fig. (6.2). The various disintegrations take place soon after each other in a cosmological sense.

For a function that asymptotically approaches a constant, such as $\rho_1(a)$ or $\rho_2(a)$, a point of inflection allows the function to have an arbitrarily large slope for a portion of the domain and still increase monotonically. A point of inflection is present in all the parameterizations of $\rho_1(a)$ and $\rho_2(a)$ and their derivatives in this letter and it allows them to fit the supernova data (which require the densities to have a very small slope over the relevant portion of a) and still reach a high density in a relatively short time. However, the relevant quantity that determines when a structure dissociates is F_{inert}, which is proportional to $2\rho(a) + \rho'(a)a$. This combination of terms is responsible for any local maxima in F_{inert}, not merely ρ or ρ'. An example of a model that has an inflection in $\rho'_{DE}(a)$ but none in $\rho_{DE}(a)$ is given by $\rho_{DE}(a) = \alpha(a - \ln[1 + e^{a-C}])$, where $\alpha, C > 0$ are constants. Such a model has a local maximum in F_{inert} and if we shift by D, where $D > C$ is a constant, neither the resulting $\rho_{DE}(a + D)$ nor its derivative has an inflection point, but the resulting F_{inert} still has a local maximum.

It is amusing to take examples of Model 2 which are more extreme than the ones illustrated. It is possible to design a pseudo-rip model such that disintegrations happen arbitrarily soon after the present time while still maintaining excellent fits to the supernova data. The Sun may not rise tomorrow.

This is a dramatic illustration of the fact that any amount of observational data, necessarily restricted to the past lightcone and necessarily with non-zero errors, cannot predict anything mathematically about the future even one hour hence without further assumptions. It is also a display of the difference between mathematics and physics: the physicist necessarily employs intuition about the real world.

The earliest support for cosmological futures such as the big rip, little rip, or pseudo-rip might come from the Planck satellite. If the dark energy equation of

state emerges with $w < -1$, it will be a shot in the arm for such exotic ideas.

It will also lend new understanding of the nature of time and perhaps the beginning and possible cyclicity of the universe.

Chapter 7

Conclusions and Future Directions

We have presented different approaches modeling dark matter and dark energy. We explored the implications of intermediate-mass black holes as dark matter and dark energy models with non-constant densities. We have categorized and discussed all possible fates of the universe for non-monotonic dark energy density, and we presented particular parameterizations and models for these categories.

Continuing to pursue the viability of intermediate-mass black holes as dark matter in earnest would require consistency checks with other observational data sources. For example, some of the best evidence for dark matter versus modified gravity comes from observations of the Bullet Cluster, a galaxy cluster which is the result of the collision of two other galaxy clusters [90]. X-ray and gravitational lensing data show that the baryonic matter from the two interacted, but the dark matter from the clusters passed right through largely without interaction. Therefore, the ideal dark matter candidate should be almost completely collisionless so that this is possible. However, the opposite outcome happened in another cluster merger called Abell 520 [91]. In Abell 520, most of the visible matter is on the edges of the cluster, while the dark matter is in the core of the cluster. The dark matter did not follow the visible matter as expected from the observations of the Bullet Cluster. Reconciling these two cluster mergers would mean that, perhaps,

the weak lensing data for Abell 520 is inaccurate, the dark matter in Abell 520 is self-interacting, or exceptionally dim galaxies with few stars are in the core. One future direction of research concerning black holes as dark matter would be determining the properties of black holes that would agree with the constraints from such observations of clusters.

Along with intermediate-mass black holes, primordial black holes in general and ultracompact minihalos (UCMHs) [21, 22] could also contribute to dark matter. UCMHs, like PBHs, are produced by density perturbations in the early universe, and such objects are overall more likely than PBHs to be formed by these perturbations. It may be fruitful to see what effects such candidates would have in structure formation simulations. The particulars of the density perturbations in the early universe in general depend on inflation. It would be worthwhile to look at particular models of inflation and how they can enhance the formation of PBHs and UCMHs (for example, [92, 93]). One would also need to determine how significant their effects on early star and galaxy formation are and if these effects are consistent with data constraints.

One possible area of future research in models of non-constant dark energy density models is dark radiation. Recent measurements of fluctuations of the cosmic microwave background imply that the effective number of neutrino families is approximately four instead of the conventional value of three [24]. Possible explanations for this extra relativistic component, called dark radiation, include sterile neutrinos, axions, gravitational waves, extra dimensions, and early dark energy [94]. This possible manifestation of dark energy could be explored, and particular models could be constrained by data. The Planck satellite, for which data will be released to the public in March 2013, should provide more precise data that will reveal more of the true nature of dark radiation.

In [77], the big rip is utilized to create a model that produces a cyclic universe. The big rip is necessary in the model in that it rips apart all bound structures in a finite time. Since the little rip and pseudo-rip can also accomplish this, another future pursuit is testing the viability of the formation of a cyclic universe using the little rip or pseudo-rip, as a basis for the turnaround between the expansion and contraction of eras, instead of the big rip.

Dark matter and dark energy are two of the biggest enigmas in our universe, and the quest to understand them is a worthwhile venture. All possible models should be explored and tested against data constraints. Understanding the nature of dark matter and dark energy will help us to understand the physics of our universe better. Perhaps our knowledge of these phenomena will remain incomplete until we are able to understand the quantum nature of gravity. Cosmological observations are becoming more and more precise, and we are hopeful that the nature of dark matter and dark energy will be more clearly known in the future.

Bibliography

[1] A. Einstein, "Kosmologische Betrachtungen zur allgemeinen Relativitätstheorie", Sitzungsberichte der Preußischen Akademie der Wissenschaften, 142 (1917).

[2] A. Friedmann, Z. Phys. **10,** 377 (1922).

[3] G. Lemaître, Ann. Soc. Sci. Bruxelles **47A,** 49 (1927).

[4] H. P. Robertson, Astrophys. J. **82,** 284 (1935); *ibid* **83,** 187 (1936); *ibid* **83,** 257 (1936).

[5] A. G. Walker, Proc. London Math. Soc. **42,** 90 (1937).

[6] E. Hubble, Proc. of the Nat. Acad. of Sci. **15**, 168 (1929).

[7] A. A. Penzias and R. W. Wilson, Astrophys. J. **142**, 419 (1965).

[8] R. A. Alpher and R. C. Herman, Phys. Rev. **74**, 1737 (1948).

[9] D. J. Fixsen, Astrophys. J. **707**, 916 (2009).

[10] F. Zwicky, Helvetica Physica Acta **6**, 110 (1933).

[11] V. Rubin, N. Thonnard, W. K. Ford, Jr, Astrophys. J. **238**, 471 (1980).

[12] A. G. Riess *et al.*, Astronomical J. **116**, 1009 (1998).

[13] S. Perlmutter *et al.*, Astrophys. J. **517**, 565 (1999).

[14] R. H. Cyburt, Phys. Rev. D **70**, 023505 (2004).

[15] A. Boyarsky *et al.*, JCAP **005**: 012 (2009).

[16] G. Steigman and M. S. Turner, Nucl. Phys. B **253**, 375 (1985).

[17] D. Larson *et al.*, Astrophys. J. Suppl. **192**, 16 (2011).

[18] S. Dodelson and L. M. Widrow, Phys. Rev. Lett. **72**, 17 (1994).

[19] M. Lovell *et al.*, Mon. Not. Roy. Astr. Soc. **420**, 2318 (2012).

[20] B. J. Carr *et al.*, Phys. Rev. D **81**, 104019 (2010).

[21] M. Ricotti, J. P. Ostriker, and K. J. Mack, Astrophys. J. **680**, 829 (2008).

[22] M. Ricotti and A. Gould, Astrophys. J. **707**, 979 (2009).

[23] W. de Sitter, Proc. Kon. Ned. Acad. Wet. **19**, 1217 (1917);
W. de Sitter, Proc. Kon. Ned. Acad. Wet. **20**, 229 (1917).

[24] G. Hinshaw *et al.*, `arXiv:1212.5226v2 [astro-ph.CO]`. Submitted to Astrophys. J. Suppl.

[25] P. A. R. Ade *et al.*, `arXiv:1303.5076 [astro-ph.CO]`. Submitted to Astron. & Atrophys.

[26] S. M. Carroll, M. Hoffman, and M. Trodden, Phys. Rev. D **68** 023509 (2003).

[27] J. M. Cline, S. Jeon, and G. D. Moore, Phys. Rev. D **70**, 043543 (2004).

[28] R. R. Caldwell, Phys. Lett. B **545**, 23 (2002).

[29] R. R. Caldwell, M. Kamionkowski, and N. N. Weinberg, Phys. Rev. Lett. **91**, 071301 (2003).

[30] P. H. Frampton and K. J. Ludwick, Astropart. Phys. **34**, 617 (2011).

[31] C. Alcock *et al.*, Astrophys. J. **486,** 697 (1997).

[32] C. Alcock *et al.*, Astrophys. J. **542,** 281 (2000).

[33] G. H. Xu and J. P. Ostriker, Astrophys. J. **437,** 184 (1994).

[34] J. Yoo, J. Chaname, and A. Gould, Astrophys. J. **601,** 311 (2004).

[35] D. P. Quinn *et al.*, Mon. Not. Roy. Astr. Soc. **396**, L11 (2009).

[36] P. H. Frampton, JCAP **10**: 016 (2009).

[37] L. Parker, Phys. Rev. **183,** 1057 (1969).

[38] J. D. Bekenstein, Phys. Rev. D **7,** 2333 (1973).

[39] S. W. Hawking, Commun. Math. Phys. **43,** 1974 (1975).

[40] G. 't Hooft, *Salamfestschrift*, editors: A. Ali, J. Ellis, and S. Randjbar-Daemi, World Scientific: vol. 4, p. 284 (1994). `arXiv:gr-qc/9310026`.

[41] P. Madau, private communication (2009).

[42] P. H. Frampton and K. J. Ludwick, Eur. Phys. J. C **71**, 1735 (2011).

[43] C. L. Bennett *et al.*, Astrophys. J. Suppl. **192,** 17 (2011).

[44] F. Y. Wang and Z. G. Dai, Chin. J. Astron. Astrophys. **6,** 561 (2006).

[45] M. Chevallier and D. Polarski, Int. J. Mod. Phys. D **10,** 213 (2001).

[46] E. V. Linder, Phys. Rev. Lett. **90,** 091301 (2003).

[47] A. Shafieloo, V. Sahni, and A. A. Starobinsky, Phys. Rev. D **80,** 101301(R) (2009).

[48] J.-M. Virey *et al*, Phys. Rev. D **70,** 121301 (2004).

[49] D. Sarkar *et al*, Phys. Rev. Lett. **100,** 241302 (2008).

[50] P. Serra *et al*, Phys. Rev. D **80,** 121302(R) (2009).

[51] R. A. Daly and S. G. Diorovski, Astrophys. J. **597,** 9 (2003).

[52] P. J. Steinhardt and D. Wesley, Phys. Rev. D **79,** 104026 (2009).

[53] P. H. Frampton, Mod. Phys. Lett. A **19,** 801 (2004).

[54] C. M. Will, *Was Einstein Right? Putting General Relativity to the Test*, Basic Books (1993).

[55] P. H. Frampton, Kevin J. Ludwick, R. J. Scherrer, Phys. Rev. D **84**, 063003 (2011).

[56] R. A. Knop *et al.*, Astrophys. J. **598**, 102 (2003).

[57] A. G. Riess *et al.*, Astrophys. J. **607**, 665 (2004).

[58] E. J. Copeland, M. Sami, and S. Tsujikawa, Int. J. Mod. Phys. D **15**, 1753 (2006).

[59] P. H. Frampton and T. Takahashi, Phys. Lett. B **557**, 135 (2003).

[60] S. Nesseris and L. Perivolaropoulos, Phys. Rev. D **70**, 123529 (2004).

[61] R. J. Scherrer, Phys. Rev. D **71**, 063519 (2005).

[62] S. Nojiri, S. D. Odintsov, and S. Tsujikawa, Phys. Rev. D **71**, 063004 (2005).

[63] S. Nojiri and S. D. Odintsov, Phys. Rev. D **72**, 023003 (2005).

[64] H. Stefancic, Phys. Rev. D **71**, 084024 (2005).

[65] J. Hao and X. Li, Phys. Rev. D **70**, 043529 (2004).

[66] M. Sami and A. Toporensky, Mod. Phys. Lett. A **19**, 1509 (2004).

[67] V. Faraoni, Class. Quant. Grav. **22**, 3235 (2005).

[68] J. Kujat, R. J. Scherrer, and A. A. Sen, Phys. Rev. D **74**, 083501 (2006).

[69] J. D. Barrow, Class. Quant. Grav. **21**, L79 (2004).

[70] J. D. Barrow, Class. Quant. Grav. **21**, 5619 (2004).

[71] C. Cattoen and M. Visser, Class. Quant. Grav. **22**, 4913 (2005).

[72] J. D. Barrow and S. Z. W. Lip, Phys. Rev. D **80**, 043518 (2009).

[73] J. D. Barrow, Class. Quant. Grav. **13**, 2965 (1996).

[74] R. Amanullah *et al.* , Astrophys. J., **716,** 712 (2010).

[75] E. Komatsu *et al.*, Astrophys. J. Suppl. **192**, 18 (2011).

[76] K. P. Schröder and R. C. Smith, Mon. Not. Royal Astron. Soc. **386,** 155 (2008).

[77] L. Baum and P. H. Frampton, Phys Rev. Lett. **98,** 071301 (2007).

[78] P. H. Frampton, K. J. Ludwick, S. Nojiri, S. D. Odintsov, and R. J. Scherrer, Phys. Lett. B **708**, 204 (2012).

[79] D. N. Spergel *et al.*, Astrophys. J. Suppl. **148**, 175 (2003);
D. N. Spergel *et al.*, Astrophys. J. Suppl. **170**, 377 (2007);
E. Komatsu *et al.*, Astrophys. J. Suppl. **180**, 330 (2009).

[80] L. Miao *et al.*, Commun. Theor. Phys. **56**, 525 (2011).

[81] S. Nojiri and S. D. Odintsov, Phys. Lett. B **686**, 44 (2010).

[82] E. Elizalde, S. Nojiri and S. D. Odintsov, Phys. Rev. D **70**, 043539 (2004).

[83] K. Bamba, S. Nojiri and S. D. Odintsov, JCAP **0810**: 045 (2008);
S. Nojiri and S. D. Odintsov, Phys. Rept. **505** 59 (2011).

[84] H. Stefancic, Phys. Rev. D **71**, 124036 (2005).

[85] S. Nojiri and S. D. Odintsov, Gen. Rel. Grav. **38**, 1285 (2006).

[86] I. Brevik, E. Elizalde, S. Nojiri, S. D. Odintsov, Phys. Rev. D **84**, 103508 (2011).

[87] P. H. Frampton, K. J. Ludwick, and R. J. Scherrer, Phys. Rev. D **85**, 083001 (2012).

[88] M. Kowalski *et al.*, Astrophys. J. **686**, 749 (2008).

[89] M. Hicken *et al.*, Astrophys. J. **700**, 1097 (2009).

[90] D. Clowe *et al.*, Astrophys. J. **648**, L109 (2006);
M. Bradac *et al.*, Astrophys. J. **652**, 937 (2006).

[91] A. Mahdavi *et al.*, Astrophys. J. **668**, 806 (2007).

[92] P. H. Frampton *et al.*, JCAP **04**: 023 (2010).

[93] D. H. Lyth, JCAP **05**: 022 (2012).

[94] M. Archidiacono, E. Calabrese, and A. Melchiorri, Phys. Rev. D **84**, 123008 (2011).